# NATIONAL ADVISORY COMMITTEE
# FOR AERONAUTICS

## TECHNICAL NOTE 4180

INVESTIGATION OF SPOILERS AT A MACH

NUMBER OF 1.93 TO DETERMINE THE EFFECTS OF HEIGHT

AND CHORDWISE LOCATION ON THE SECTION AERODYNAMIC

CHARACTERISTICS OF A TWO-DIMENSIONAL WING

By James N. Mueller

Langley Aeronautical Laboratory
Langley Field, Va.

NACA

Washington
February 1958

NATIONAL ADVISORY COMMITTEE FOR AERONAUTICS

TECHNICAL NOTE 4180

INVESTIGATION OF SPOILERS AT A MACH

NUMBER OF 1.93 TO DETERMINE THE EFFECTS OF HEIGHT

AND CHORDWISE LOCATION ON THE SECTION AERODYNAMIC

CHARACTERISTICS OF A TWO-DIMENSIONAL WING[1]

By James N. Mueller

SUMMARY

An investigation of spoilers has been made at a Mach number of 1.93 to determine the effects of height and chordwise location on the section pressure distributions and section aerodynamic characteristics of a two-dimensional, 6-percent-thick, symmetrical wing. Spoilers with heights of 0.03, 0.05, and 0.07 chord were tested at chordwise locations of 0.41, 0.53, and 0.70 chord at a Reynolds number of approximately $1 \times 10^6$.

An analysis of the data indicated that the spoiler with a height of 0.03 chord produced only small changes in the wing-section aerodynamic characteristics from those of the wing with no spoiler. The spoiler height of 0.05 chord appeared to be the optimum height, as compared with its increased effectiveness over that of the spoiler height of 0.03 chord and the large drag rise associated with the spoiler height of 0.07 chord. The most effective spoiler location was the most forward position (0.41 chord), where the spoiler influenced a flow region of reduced local Mach number. The most rearward spoiler, located at 0.07 chord, had the least center-of-pressure travel and the lowest drag rise with increasing spoiler height and angle of attack. The result of fixed transition near the leading edge was a slight increase in the effectiveness of the spoiler when the spoiler was located at the most rearward chordwise location.

The experimental chordwise points of boundary-layer separation from the wing surface forward of and due to the presence of a spoiler were compared with previous separation data as correlated in NACA TN 3065. Good agreement was shown when the boundary layer was turbulent. The theoretical pressure distribution computed on the basis of the separation profile thus determined was in good agreement with the experimental results.

---

[1]Supersedes recently declassified NACA Research Memorandum L52L31 by James N. Mueller, 1953.

## INTRODUCTION

The problem of providing adequate control for vehicles flying at transonic and supersonic speeds is currently of paramount concern. Conventional flap-type controls used on thin wings at high speeds present serious problems of wing twist and, consequently, low aileron reversal speeds; in addition, controls of this type are characterized by high hinge moments.

Among the more promising types of control devices being investigated are spoilers which can offer desirable characteristics not always found in flaps: namely, high control effectiveness at transonic speeds, low control forces, and low wing-twisting moments. At present, adequate theory is not available for predicting spoiler characteristics; therefore, experimental investigations must be undertaken to obtain such information. To supplement the exploratory work already done on spoilers at transonic and supersonic speeds (refs. 1 to 6), an investigation of spoilers by means of pressure distributions and schlieren observations has been undertaken to determine the effects on the wing-section aerodynamic characteristics of height, chordwise location, and fixed transition near the leading edge. A two-dimensional wing having a thickness of 6-percent chord and a symmetrical profile, which consisted of a slab-type section with a double-wedge nose and blunt trailing edge, was used in the investigation. Spoilers with heights of 0.03, 0.05, and 0.07 chord were tested at chordwise stations of 0.41, 0.53, and 0.70 chord at angles of attack of $0°$, $±5°$, and $±10°$.

The tests were made in the Langley 9-inch supersonic tunnel at a Mach number of 1.93 and a Reynolds number of $1.03 \times 10^6$. A few additional tests, however, were made at a Reynolds number of $1.87 \times 10^6$.

## SYMBOLS

$p_l$        local static pressure

$p$         stream static pressure

$M$         stream Mach number

$\gamma$         ratio of specific heats for air (1.4)

$q$         stream dynamic pressure, $\frac{\gamma}{2} M^2 p$

| | | |
|---|---|---|
| P | pressure coefficient, | $\dfrac{p_l - p}{q}$ |

c      wing chord

n      section normal force; positive upwards

m      section pitching moment about midchord; positive when it tends to rotate the leading edge of airfoil upward

d      section pressure drag; positive rearward

$c_n$      section normal-force coefficient, $n/qc$

$c_m$      section pitching-moment coefficient, $m/qc^2$

$c_d$      section pressure-drag coefficient, $d/qc$

t      maximum thickness of wing

h      spoiler height above wing surface

$l$      chordwise distance of spoiler from wing leading edge

$h/c$      ratio of spoiler height to wing chord

$l/c$      chordwise distance of spoiler from wing leading edge in terms of wing chord

$x/c$      chordwise distance from wing leading edge in terms of wing chord

R      Reynolds number, $\rho V c/\mu$

$\rho$      mass density of free stream

$c_{m_\alpha}$      rate of change of pitching-moment coefficient with angle of attack

$c_{n_\alpha}$      rate of change of normal-force coefficient with angle of attack

V      free-stream velocity

$\mu$            absolute coefficient of viscosity

$\alpha$            wing angle of attack

$\Delta c_n$          incremental normal-force coefficient due to spoiler projection

$\Delta c_m$          incremental pitching-moment coefficient due to spoiler pro-
                jection

$\Delta c_d$          incremental pressure-drag coefficient due to spoiler pro-
                jection

## APPARATUS AND METHODS

### Wind Tunnel

The investigation was made in the Langley 9-inch supersonic tunnel which is a closed-return type of tunnel having provision for the control of the humidity and pressure. Eleven fine-mesh turbulence-damping screens are installed in the settling chamber ahead of the nozzles. For qualitative-flow observations, a schlieren optical system is provided. During the tests, the quantity of water vapor in the tunnel air was kept sufficiently low so that the effects of condensation in the supersonic nozzle were negligible.

### Models

Two models were used in the investigation: a pressure-distribution model for pressure measurements and a schlieren model for visual-flow observations. These models and their methods of installation in the tunnel are shown in figures 1 and 2, respectively. Both models had 3-inch chords and rectangular plan forms. As shown in figure 1, the profile of the wing consisted of a slab-type section with a sharp double-wedge nose and blunt trailing edge. The thickness ratio of the wings was 6 percent, and the included angle between the upper and lower surfaces at the leading edge was 11.4°. The wings were machined from steel and highly polished with the leading edges ground to a thickness of less than 0.002 inch. All contours were cut to within 0.002 inch of the specified values.

For convenience in carrying the pressure leads from the pressure-distribution model (fig. 1) to the outside of the tunnel and in setting angles of attack, the model was mounted in the tunnel directly from circular end plates which replaced the tunnel observation windows. The model was equipped with 25 static-pressure orifices arranged in a chordwise

row at the midspan station. Only one surface of the wing was equipped with orifices. The orifices were 0.014 inch in diameter and were drilled perpendicular to the wing surface. All pressure leads from the orifices were ducted to the outside of the tunnel within the model and steel supporting plates.

The transition strip used in the investigation was prepared from common table salt. The approximate location of this strip is shown in figure 1, and its chordwise dimension was about 3/16 inch.

Figure 2 shows the schlieren model mounted for visual-flow observations. The model was supported by two struts which in turn were attached to support trunnions. The angle of attack of the model was changed by rotating the support trunnions. The span of the model was slightly less than the tunnel width in order to permit model movement in the pitch direction without damaging the observation windows.

The spoilers used in the investigation (a typical example is shown on the dimensional sketch of fig. 1) were made from strips of 0.030-inch-thick sheet brass bent to give the desired spoiler heights. The spoilers were anchored to the wing surface by means of screws, and the spoiler base rested firmly on the wing surface. A center section of the spoiler anchor flange was removed to permit utilization of the maximum number of wing pressure orifices (see fig. 1). Spoilers for the schlieren wing were identical to those of the pressure-distribution wings, excluding the anchor flange cutouts.

### Pressure Measurements and Reduction of Data

The pressures on the wing and the total pressure in the tunnel settling chamber were recorded simultaneously by photographing a multiple-tube mercury manometer on which the pressures were indicated. Subsequently, the pressures were read directly from the film as pressure coefficients with the use of a film reader.

The pressure-distribution data were converted into section aerodynamic coefficients $c_n$ and $c_m$ by using electronic calculating equipment. A comparison between data converted by electronic calculating equipment and those converted by the standard practice of mechanically integrating the faired pressure-distribution curves with a planimeter showed the agreement between the two methods to be within the experimental accuracy of the data. Values of section pressure-drag coefficients $c_d$ were obtained by using a combination of both methods.

## Test Methods and Range of Tests

During the investigation, pressure distributions and schlieren photo-graphs were obtained of the various wing-spoiler configurations by varying the angles of attack of the configurations through the desired range. Pressure-distribution data were also obtained on the wing alone (without spoiler) through the same angle-of-attack range. As a result of the fact that the wing was equipped with pressure orifices on only one surface, pressure distributions obtained with and without the spoiler were combined to form the complete pressure diagrams such as those shown in figures 3, 4, and 5, inclusive. It was possible to change the angles of attack of the pressure-distribution and schlieren models while the tunnel was in operation. The angle of attack of the pressure-distribution model was measured by means of a clinometer attached to one of the circular end plates (previously described). The angle of attack of the schlieren model was set with the aid of a cathetometer. All schlieren photographs were obtained with the knife edge horizontal.

Pressure-distribution tests were made at angles of attack of $0°$, $\pm 5°$, and $\pm 10°$. The highest negative angle of attack was impossible to reach for certain spoiler heights and chordwise locations because of tunnel choking. Tests were made for spoiler heights of 0.03, 0.05, and 0.07 chord at chordwise locations of 0.41, 0.53, and 0.70 chord. In addition, limited tests were made with a transition strip near the leading edge of the wing.

Schlieren photographs were obtained over approximately the same range of angle of attack and spoiler configuration as the pressure-distribution tests.

The majority of the tests were made at a Reynolds number of $1.03 \times 10^6$, based on a tunnel settling-chamber pressure of 1 atmosphere. A few additional tests, however, were made at a tunnel settling-chamber pressure of 2 atmospheres. All tests were made at a Mach number of 1.93.

## Precision of Measurements

Stream surveys obtained with the test section empty indicate that the mean value of the Mach number in the region occupied by the test models is 1.93 and that the variation about this mean value is less than 1 percent. There was no evidence of any large irregularities in stream flow direction. For the pressure-distribution model, the angle-of-attack settings are believed to be accurate within $\pm 0.10°$. For the schlieren model, the angle setting is considered to be somewhat less accurate, or within about $\pm 0.25°$.

Individual pressure coefficients are usually accurate within $\pm 0.01$, and consistent discrepancies of greater magnitude are not caused by errors in reading pressures but by local surface irregularities. These discrepancies in pressure coefficients were deliberately neglected in fairing the experimental curves. The accuracy of the aerodynamic coefficients was usually better than $\pm 0.01$ in $c_n$, $\pm 0.002$ in $c_m$, and $\pm 0.005$ in $c_d$. Spoiler heights are believed to be accurate within $\pm 0.0017c$.

RESULTS AND DISCUSSION

Pressure Distributions

Figures 3, 4, and 5 present representative groups of experimental pressure distributions obtained over the wing equipped with plain spoilers. These figures show, respectively, the effects of spoiler height, the effects of spoiler chordwise location, and the effects of fixed transition. Included in figures 3, 4, and 5 are theoretical pressure distributions calculated from shock-expansion theory for the wing without spoiler. Figures 6 to 9 are supplementary schlieren photographs and shadowgraphs depicting some elements of the flow phenomena over the wing-spoiler configurations.

General.- Comparative examinations disclosed, generally, good agreement between the experimental and theoretical wing pressures excluding, of course, those wing pressures affected by the presence of the spoiler.

An inspection of the experimental pressure distributions revealed that each one is characterized by a region (defined herein as the area on the pressure diagrams enclosed between the experimental curve and the corresponding theoretical curve) of flow compression ahead of the spoiler and a flow-expansion region behind the spoiler. It thus appeared that the character of the flow in the presence of the spoiler is analagous to that which would develop in the presence of a half-wedge (attached to the wing), whose thickness increased in a chordwise direction until its maximum thickness equaled that of the spoiler height and coincided with the spoiler location. (This fact was observed and reported in ref. 1.) It was also seen that the regions of flow compression outweigh the expansion regions for every spoiler configuration at all angles of attack. This result caused a normal-force decrement or deficiency over that of the wing without spoiler, with the magnitude dependent upon such factors as spoiler height, spoiler chordwise location, and state (laminar or turbulent) of the boundary layer.

Effect of spoiler height.- At the forward spoiler station and negative angle of attack $(\alpha = -5^\circ)$, figure 3(a), the principal effects observed with increase in spoiler height were the rapid enlargement of

the compression region ahead of the spoiler and the comparatively slow growth of the expansion region behind the spoiler. Corresponding schlieren pictures of the flow phenomena, figure 6(a), show the increased intensity of the compression manifested in the main shock wave located just forward of the spoiler as the spoiler height is increased from 0.03 chord to 0.05 chord. The expansion of the flow over the lip and rearward of the spoiler is difficult to see on the photographs of figure 6(a) but is plainly visible on figure 7 which shows shadowgraphs of the flow over the wing equipped with a spoiler having a height of 0.05 chord.

An increase in angle of attack to $\alpha = 5^\circ$, figure 3(a), curtailed somewhat the magnitude and rate of enlargement of the compression region. It is interesting to note that, as the spoiler height increased, the ensuing enlargements of the compression regions acted in a manner to reduce the net positive normal force ahead of the spoiler, and, at a spoiler height of 0.07 chord, the normal force appeared to be near zero. Figure 6(a) shows the flow phenomena for the three spoiler heights at several angles of attack. At $\alpha = 5^\circ$ it can be seen that the shock-wave strength forward of the spoiler is considerably reduced, as compared with that at $\alpha = -5^\circ$. The expansion regions rearward of the spoiler (fig. 3(a)) decreased with angle of attack (approximately one-half that at $\alpha = -5^\circ$); however, there was a slight increase with spoiler height which resulted in a slight increase in normal force on the wing to the rear of the spoiler.

Also apparent in figure 3(a) is the extent of the forward chordwise spoiler influence which, with the exception of the spoiler having a height of 0.03 chord at $\alpha = 5^\circ$, reaches to the leading edge of the wing.

When the spoiler was located at the rearward station, figure 3(b), the magnitude of the pressures in the compression region was less, and the compression-region increase with spoiler height was not as abrupt as at the forward chordwise spoiler station. The gradual increase was caused by the flow undergoing a two-phase compression, which is easily seen on the pressure diagram for $\alpha = 5^\circ$ and $h/c = 0.07$. Figure 6(b) gives corresponding schlieren photographs of the flow, and a shock is seen to occur for each phase of the pressure rise. The abrupt increase in pressure which took place immediately forward of the spoiler face was probably a result of stagnation of the circulation in the essentially dead-air region.

Significant features observed at this spoiler station ($l/c = 0.70$) were the increased magnitudes and faster rate of growth of the expansion regions with increase in spoiler height over those at the forward station. Essentially, the expansion regions act to reduce the efficiency of the spoiler by increasing the lift on the wing; thus, it is desirable that they remain small. The expansion over the spoiler can be seen in figure 7.

The effects of angle of attack on the pressure distributions are essentially the same as those at the forward station.

The extent of the forward chordwise influence of the rearward-located spoiler on the wing pressures depended upon spoiler height and varied from 0.30 to 0.40 to 0.70 chord for spoiler heights of 0.03, 0.05, and 0.07 chord, respectively, for both $\alpha = -5^{O}$ and $\alpha = 5^{O}$. (See fig. 3(b).) It appears, therefore, that the forward chordwise extent of the spoiler influence on the wing pressures is independent of angle of attack at the rearward ($l/c = 0.70$) spoiler station.

Effect of spoiler chordwise location.- Figure 4 shows the effects of varying the chordwise location of the spoiler on the pressure distributions over the wing for two spoiler heights and two angles of attack.

At the smaller spoiler height, $h/c = 0.03$, and both angles of attack, figure 4(a), the principal change which occurred with rearward chordwise movement of the spoiler appeared to be a chordwise redistribution of the load on the wing with a net change, if any, in normal force being negligibly small. Corresponding schlieren photographs of the flow are shown in figure 8(a), and the chief variation which occurs as the spoiler is moved rearward is in the character of the shock-wave pattern which changed from a one-shock to a two-shock type of pattern forward of the spoiler. (These shock phenomena were discussed previously in more detail.)

At the larger spoiler height and at $\alpha = -5^{O}$, figure 4(b), the magnitudes of the normal force ahead of the spoiler appeared to be approximately equal at both spoiler positions shown. However, it is interesting to note that rearward of the spoiler the net normal force is seen to change from a negative value to a positive value as the spoiler moves from the 0.53c station rearward to the 0.70c station. This condition results from the fact that the recompression of the flow, after it has expanded around the spoiler, is interrupted because of the proximity of the spoiler to the wing trailing edge.

The effect of increasing the angle of attack to $\alpha = 5^{O}$ was a decrease in the magnitudes of the compression and expansion regions at all spoiler stations. Figure 8(b) shows corresponding schlieren photographs of the flow and illustrates the change in the shock-wave pattern from a one-shock to a two-shock type of pattern as the spoiler is moved rearward on the wing.

Effects of fixed transition.- Figure 5 shows the effects of fixed transition on the pressure distributions over the wing equipped with a 0.05c-height spoiler for two chordwise spoiler locations and several angles of attack. The left side of the figure shows the pressure distributions for a smooth wing (no transition strip), and the right side shows corresponding pressure distributions with transition fixed.

When the spoiler was located at the forward chordwise station ($l/c = 0.41$), figure 5(a), the addition of a fixed transition strip to the wing caused no significant change in the pressure distributions over the wing. An explanation for the negligible change in the pressure distributions may be attributed to the fact that the flow is probably separated ahead of the transition strip, which is thereby rendered ineffective for this particular spoiler height and location. Figure 9(a) shows corresponding schlieren photographs of the flow over the wing with and without fixed transition, and it can be seen that the flow phenomena (shock-wave patterns) are almost identical.

On the other hand, when the spoiler was located at the 0.70 chord station, figure 5(b), the addition of a fixed transition strip greatly restricted the forward chordwise influence of the spoiler on the wing pressures. This condition results from the fact that when the boundary layer is turbulent the point of initial flow separation is moved considerably rearward. (See fig. 9(b).) Although the forward chordwise influence of the spoiler was curtailed, the magnitudes of the pressures in the compression region forward of the spoiler were considerably greater than those for the smooth wing since the more rearward location of the initial point of flow separation necessitates a stronger shock. Rearward of the spoiler, it was seen that the magnitudes of the expansion regions for the fixed transition case are somewhat less (especially at $\alpha = -5^\circ$ and $\alpha = 5^\circ$) than those for the smooth wing; thus, there was a slight decrease in positive normal force rearward of the spoiler for the case of fixed transition.

Figure 10 is a composite illustration which shows by means of schlieren photographs, sketches, and experimental pressure distributions the flow phenomena over the wing equipped with a spoiler having a height of 0.05 chord located at the 0.70c wing station for both laminar and turbulent boundary layers. The principal difference between the two types of flow was the retardation of flow separation from the wing forward of the spoiler when the boundary layer is turbulent. (Compare the experimental pressure distributions of figs. 10(a) and 10(b).) Further examination of the experimental pressure distributions revealed the characteristic two-phase pressure rise forward of the spoiler for the laminar boundary-layer flow as shown in figure 10(a). The locations of the two shock waves, one (separation shock) near the wing shoulder and the other (main shock) slightly forward of the spoiler as seen on the corresponding schlieren photograph of figure 10(a), agreed well with the chordwise locations of the pressure increases. When the boundary layer was made turbulent, the flow adhered to the wing surface for a considerably greater chordwise distance before it broke away sharply from the wing and formed a strong shock which can be seen on the schlieren photograph of figure 10(b). The pressure rise beneath the foot of the shock was very large and abrupt, as seen on the experimental pressure distribution shown below the schlieren photograph. The secondary small increase in pressure near

the spoiler face was very likely a result of stagnation of the circulation in the essentially dead-air region and can be seen on the experimental pressure-distribution diagrams for both laminar and turbulent boundary layer.


## Aerodynamic Characteristics

Effect of spoiler height.- Figure 11(a) shows the variation of section normal-force coefficient with $\alpha$ for three spoiler heights and two spoiler chordwise locations. The curves exhibited linear variations with angle of attack at all spoiler heights and at each spoiler location. The slopes of the curves $c_{n_\alpha}$ remained essentially constant (within 3 percent) for all spoiler heights; however, there was a successive downward displacement (normal-force decrement) of the curves as the height of the spoilers increased. The displacement between the curves of the 0.03c- and 0.05c-height spoilers was roughly twice that between the curves of the 0.05c- and 0.07c-height spoilers when the spoilers were located at the most forward ($l/c = 0.41$) chordwise location. This result would appear to indicate that the small gain in normal-force decrement obtained by increasing the spoiler height from 0.05c to 0.07c may not be advantageous in the light of the large drag-rise penalty which would accompany the larger-height spoiler. The displacement of the curves with spoiler height was fairly uniform and approximately of equal magnitude when the spoilers were located at the 0.70c spoiler station.

The variation of normal force with spoiler height at constant angle of attack and two chordwise spoiler locations is shown in figure 11(b). At both spoiler stations the spoiler effectiveness parameter $dc_n/d\frac{h}{c}$ remained fairly constant with change in angle of attack. The variation of normal force with spoiler height was essentially linear for the range of angle of attack tested.

Figure 12(a) shows the variation of the pitching-moment coefficient with angle of attack for three spoiler heights and two chordwise locations. All the curves show good linearity over the angle-of-attack range of the tests. As the spoiler height was increased from 0.03c to 0.07c, the rate of change of pitching-moment coefficient with angle of attack $c_{m_\alpha}$ increased approximately 35 percent at both the forward and rearward spoiler stations.

Figure 12(b) shows the variation of the pitching-moment coefficient with spoiler height at constant angles of attack and two chordwise locations. The curves have been faired to have sudden changes in slopes, although it is more likely that these slope changes would take place gradually. The fairing was done in this manner because of the uncertainty involved in fairing the curves between $h/c = 0$ and $h/c = 0.03$. At the

forward spoiler station, substantial increases occurred in the spoiler
pitching effectiveness $dc_m/d\frac{h}{c}$ when the height of the spoiler increased
beyond 0.03c. For the same angles of attack and with the spoiler located
at the rearward ($l/c$ = 0.70) station, the increases were only about one-
half those at the forward station. In the spoiler-height range from 0.03c
to 0.07c, the increase in spoiler pitching effectiveness as the angle of
attack decreased from $\alpha$ = 5° to $\alpha$ = -5° was about 70 percent at the
forward spoiler station. At the rearward station the increase was
slightly over one-half that at the forward station.

Effect of spoiler location.- Figure 13(a) shows section normal-force
coefficient as a function of angle of attack for three different spoiler
chordwise locations and two spoiler heights. For a spoiler height of
0.03c, it can be seen that the effects of varying the chordwise location
of the spoiler is negligible. However, for a spoiler height of 0.07c, a
decrement in normal-force coefficient of approximately 0.025 occurred when
the spoiler was moved from the 0.70c location to the 0.53c location. An
additional forward movement of the spoiler to the $l/c$ = 0.41 station
produced an additional, though small, decrement in normal-force coeffi-
cient. This decrement in normal-force coefficient with forward chordwise
movement of the spoiler was contrary to the results of other spoiler tests,
reported in references 1 and 2, in which it was found that spoiler effec-
tiveness increased with rearward movement of the spoiler. The reason for
this discrepancy can probably be ascribed to local Mach number effects,
which in these tests are caused by the change in slope of the airfoil sur-
face. The effectiveness of the spoiler could be expected to increase in
the reduced Mach number region in the vicinity of the wedge surface of the
airfoil. It, therefore, appears that the effectiveness of the spoiler
improves as its location on the wing is moved forward. The slopes $c_{n_\alpha}$
of the curves are approximately equal and the curves are linear for all
spoiler locations.

The effects of spoiler location are shown further in figure 13(b)
where the variation of section normal-force coefficient appears as a
function of spoiler chordwise location at constant angles of attack and
for two spoiler heights. For the least (h/c = 0.03) height spoiler, the
variation of section normal force with spoiler chordwise location is
shown to be negligibly small at all angles of attack. At the greater
spoiler height (h/c = 0.07), however, the spoiler loses some of its
effectiveness as it is moved rearward along the wing.

Figure 14(a) shows the variation of the section pitching-moment
coefficient with angle of attack for several chordwise spoiler locations
and two spoiler heights. At the smaller spoiler height (h/c = 0.03), a
small increase occurred in the pitching-moment-curve slopes $c_{m_\alpha}$ as the
spoiler was moved forward on the wing. The increase (more positive) in
slope value was about 17 percent when the spoiler was moved from the

0.70c station to the 0.41c station. The curves converge at $\alpha = 10°$ and indicate that the effects of changing spoiler chordwise location may reverse at the higher angles of attack. For the larger spoiler height ($h/c = 0.07$), the pitching-moment coefficients show fairly large variations with spoiler chordwise location: for example, at the 0.41c spoiler station and $\alpha = 0°$, the pitching-moment coefficient is about twice that obtained when the spoiler is located at the 0.70c station. The increased (more negative) pitching moment at the forward (0.41c) spoiler station can be attributed to the fact that the pressure changes which occur on the wing are well forward of the wing moment center (which is at the midchord point), whereas the pressure changes which occur when the spoiler is located at the 0.70c station are in the vicinity of the wing moment center. The rate of change of pitching-moment coefficient with angle of attack $c_{m_\alpha}$ increased approximately 16 percent when the 0.07c-height spoiler was moved from the 0.70c station to the 0.41c station.

Figure 14(b) further illustrates the effects of varying spoiler chordwise location on the pitching-moment coefficients at constant angles of attack and at two spoiler heights. For the smaller spoiler height ($h/c = 0.03$), the pitching-moment variation with change in spoiler location is negligible at $\alpha = 5°$ and $\alpha = 10°$. At $\alpha = -5°$, the pitching moment of the configuration is seen to decrease slightly with rearward chordwise movement of the spoiler. At the larger spoiler height ($h/c = 0.07$), the variation of the pitching-moment coefficient with the spoiler chordwise location is very large and indicates less negative pitching moment as the spoiler is moved rearward on the wing. The pitching-moment variation with spoiler chordwise location $dc_m/d\frac{l}{c}$ for a spoiler height of 0.07c decreased approximately 40 percent when the angle of attack increased from $\alpha = -5°$ to $\alpha = 10°$.

Effects of fixed transition.- Figure 15 illustrates the effects of fixed transition near the leading edge on the normal-force and pitching-moment coefficients with the spoiler located at two chordwise stations. The effects of fixed transition on the normal-force coefficients, figure 15(a), when the spoiler is located at the forward ($l/c = 0.41$) chordwise station are negligible. This condition probably results from the fact that the flow is separating ahead of the transition strip, which is thereby rendered ineffective. On the other hand, when the spoiler is located at the rearward station ($l/c = 0.70$), the effect of fixed transition results in a small negative displacement of the normal force against angle-of-attack curve relative to that of the smooth configuration. This result indicates an increase in spoiler effectiveness as the boundary layer is made turbulent.

At both spoiler stations the pitching-moment coefficients, figure 15(b), tend to become more positive when the boundary layer is made

turbulent, and this effect is more pronounced at the rearward spoiler station. The positive increase in pitching moment is attributed to the shift in the center of pressure (fig. 16) when the boundary layer is made turbulent. It is seen (fig. 16) that, at the positive angles of attack ($\alpha = 5^\circ$ and $10^\circ$), the center of pressure moves forward, relative to that of the smooth wing. Conversely, at the negative angle of attack ($\alpha = -5^\circ$), the center of pressure moved rearward, relative to that of the smooth wing, toward the wing moment center.

Figure 16 shows the variation of the wing center of pressure with spoiler height for two chordwise locations and several angles of attack. A general observation shows that the least center-of-pressure travel is obtained when the spoiler is located at the most rearward station at $\alpha = 10^\circ$ with transition fixed and amounted to a maximum of 1 percent chord. The greatest variation of center-of-pressure location with spoiler height is shown to occur at $\alpha = -5^\circ$ when the spoiler is located at the most forward chordwise station and is approximately 17 percent chord when the curve is extrapolated to $h/c = 0.07$. Generally, at the positive angles of attack ($\alpha = 5^\circ$ and $10^\circ$), there is a rearward center-of-pressure travel with spoiler height; at $\alpha = -5^\circ$, the reverse is true. For spoiler heights between $h/c = 0$ and $0.03$, the center-of-pressure travel is negligibly small at both spoiler chordwise stations at $\alpha = 5^\circ$ and $10^\circ$; at $\alpha = -5^\circ$, however, a significant center-of-pressure travel is apparent.

Figure 17 illustrates the effects of spoiler height on the incremental section normal-force, pitching-moment, and pressure-drag coefficients for two spoiler chordwise locations and several angles of attack. Figure 17(a), obtained from figure 11(b), shows the incremental section normal-force coefficients, and, for all angles of attack, the more forward spoiler location produced the greater decrement in normal-force coefficient.

An idea of the angle-of-attack effect can be gained by comparing the normal-force decrement produced by a spoiler of 0.05c height located at the 0.70c station. As shown in figure 17(a), as the angle of attack increased from $\alpha = -5^\circ$ to $5^\circ$, a corresponding decrease occurs in normal-force decrement of approximately 30 percent. When the spoiler was located at the forward station, the corresponding loss in spoiler effectiveness $\left(d\Delta c_n / d\frac{h}{c}\right)$ was not as great and amounted to about two-thirds that at the rearward station.

Figure 17(b) (obtained from fig. 12(b)) shows the incremental pitching-moment coefficients as a function of spoiler height and it can be seen that the more forward ($l/c = 0.41$) spoiler location has the greater influence on the pitching moments, especially when the spoiler height exceeds 0.03c.

Figure 17(c) presents the incremental pressure-drag coefficient attributed to the spoiler for various wing angles of attack and two spoiler chordwise locations. The pressure-drag coefficients include the drag of the spoiler alone which is computed by using the maximum pressure immediately forward of the spoiler face and the minimum pressure to the rear of the spoiler. The incremental drag coefficient varies non-linearly with spoiler height at both chordwise spoiler locations. The drag rise with spoiler height is fairly rapid and, as might be expected, becomes more severe with decreasing angle of attack and forward movement of the spoiler. The large drag penalty incurred as the spoiler height increases from 5 to 7 percent chord, as was previously predicted, is shown.

## Shock Boundary-Layer Interaction

Spoilers affixed to wings which are moving at supersonic speeds present, essentially, a problem in shock-wave boundary-layer interaction phenomena. The projection of a spoiler from the wing surface blocks the flow to a certain extent and causes a shock wave to form which in turn is accompanied by a pressure rise. When this pressure rise across the shock exceeds a certain critical value (known as the critical pressure-rise ratio), the flow separates from the surface of the wing. Experimental investigations (refs. 7 to 10) have shown that the state of the boundary layer, that is, whether the boundary layer is laminar or turbulent, largely determines the resulting shock-wave configuration and the upstream influence of the shock wave on the boundary layer. Any further increase in pressure-rise ratio simply moves the point of flow separation forward. If the point of flow separation from an airfoil equipped with a spoiler could be predicted, it would be possible to calculate approximately the pressure distributions and subsequently the force coefficients of such a configuration.

A survey of available literature on shock-wave—boundary-layer interaction (ref. 11) presents a correlation of the results of tests to determine the pressure rise necessary to cause a boundary layer to separate as a consequence of shock-interaction effects for essentially two-dimensional flow. The results of reference 11 are believed to be applicable (for turbulent boundary-layer flow) to the present investigation of spoiler-equipped airfoils to predict the approximate chordwise location of the point of flow separation from the wing surface ahead of and due to the presence of the spoiler. Good agreement between the present experimental points of flow separation and the results of reference 11 was obtained when the boundary layer was turbulent as shown in figure 18 for various spoiler heights and chordwise locations. The values from reference 11 used in figure 18 were obtained by first calculating by the shock-expansion theory the Mach number on the wing surface to which the spoiler was attached, and then the critical pressure-rise ratio was

obtained from figure 8 of reference 11.  Once the critical pressure-rise
ratio was obtained, it was possible to determine the shock angle and,
thence, the angle  δ  through which the flow turned (see fig. 19) as it
left the surface.  Then, by drawing a line of inclination equal to  δ
from the lip of the spoiler to the wing surface, the intersection of the
line and the airfoil surface marked the chordwise point of flow separation.

Figures 19(a) and 19(b) show, respectively, a schlieren photograph
of the flow over the wing equipped with a 0.05c-height spoiler located
at the 0.70c station and the corresponding experimental pressure distri-
bution.  The boundary layer has been made turbulent in both cases by use
of the transition strip.  In figure 19(a), the apparent point of flow
separation from the wing surface is discernible and immediately below
this point, in figure 19(b), an abrupt pressure rise is seen to occur.
Figure 19(c) shows the point of flow separation as predicted by refer-
ence 11 for the wing-spoiler configuration of figures 19(a) and 19(b).
The theoretical pressure distribution computed for the configuration of
figure 19(c) is entered in figure 19(b) and is seen to be in good agree-
ment with the experimental results.

## CONCLUSIONS

The results of a pressure-distribution investigation of spoilers
made at a Mach number of 1.93 and at a Reynolds number of approximately
$1 \times 10^6$ to determine the effects of height and chordwise location on the
section aerodynamic characteristics of a two-dimensional, 6-percent-
thick, symmetrical wing have indicated the following conclusions:

1. A spoiler height of 0.03 chord produced relatively small changes
in the wing-section aerodynamic characteristics as compared with the
no-spoiler condition.  The spoiler height of 0.05 chord appeared to be
the optimum height, as compared with its increased effectiveness over
that of the spoiler height of 0.03 chord and the large drag rise asso-
ciated with the spoiler height of 0.07 chord.

2. The most effective chordwise spoiler location was the most forward
position (0.41 chord), where the spoiler influenced a flow region of reduced
local Mach number.

3. The most rearward spoiler position (0.70 chord) had the least
center-of-pressure travel and the lowest drag rise with increasing
spoiler height and angle of attack.

4. The result of fixing transition near the leading edge was to increase slightly the spoiler effectiveness when the spoiler was located at the most rearward chordwise station.

5. The experimental chordwise points of turbulent boundary-layer separation forward of and due to the presence of the spoilers were in good agreement with the results of previous flow-separation investigations as correlated in NACA TN 3065. The theoretical pressure distribution computed on the basis of the separation profile thus determined was in good agreement with the experimental results.


Langley Aeronautical Laboratory,
      National Advisory Committee for Aeronautics,
            Langley Field, Va., January 2, 1953.

REFERENCES

1. Conner, D. William, and Mitchell, Meade H., Jr.: Effects of Spoiler on Airfoil Pressure Distribution and Effects of Size and Location of Spoilers on the Aerodynamic Characteristics of a Tapered Unswept Wing of Aspect Ratio 2.5 at a Mach Number of 1.90. NACA RM L50L20, 1951.

2. Strass, H. Kurt: Additional Free-Flight Tests of the Rolling Effectiveness of Several Wing-Spoiler Arrangements at High Subsonic, Transonic, and Supersonic Speeds. NACA RM L8I23, 1948.

3. Hammond, Alexander D.: Lateral-Control Investigation of Flap-Type and Spoiler-Type Controls on a Wing With Quarter-Chord-Line Sweepback of 60°, Aspect Ratio 2, Taper Ratio 0.6, and NACA 65A006 Airfoil Section - Transonic-Bump Method. NACA RM L50E09, 1950.

4. Hammond, Alexander D., and Watson, James M.: Lateral-Control Investigation at Transonic Speeds of Retractable Spoiler and Plug-Type Spoiler-Slot Ailerons on a Tapered 60° Sweptback Wing of Aspect Ratio 2 - Transonic-Bump Method. NACA RM L52F16, 1952.

5. Schult, Eugene D., and Fields, E. M.: Free-Flight Measurements of Some Effects of Spoiler Span and Projection and Wing Flexibility on Rolling Effectiveness and Drag of Plain Spoilers on a Tapered Sweptback Wing at Mach Numbers Between 0.6 and 1.6. NACA RM L52H06a, 1952.

6. Fields, E. M.: Some Effects of Spoiler Height, Wing Flexibility, and Wing Thickness on Rolling Effectiveness and Drag of Unswept Wings at Mach Numbers Between 0.4 and 1.7. NACA RM L52H18, 1952.

7. Czarnecki, K. R., and Mueller, James N.: Investigation at Supersonic Speeds of Some of the Factors Affecting the Flow Over a Rectangular Wing With Symmetrical Circular-Arc Section and 30-Percent-Chord Trailing-Edge Flap. NACA RM L50J18, 1951.

8. Liepmann, H. W., Roshko, A., and Dhawan, S.: On Reflection of Shock Waves From Boundary Layers. NACA Rep. 1100, 1952. (Supersedes NACA TN 2334.)

9. Barry, F. W., Shapiro, A. H., and Neumann, E. P.: The Interaction of Shock Waves With Boundary Layers on a Flat Surface. Jour. Aero. Sci., vol. 18, no. 4, Apr. 1951, pp. 229-238.

10. Ackeret, J., Feldmann, F., and Rott, N.:  Investigations of Compression
    Shocks and Boundary Layers in Gases Moving at High Speed.  NACA
    TM 1113, 1947.

11. Lange, Roy H.:  Present Status of Information Relative to the Prediction
    of Shock-Induced Boundary-Layer Separation.  NACA TN 3065, 1954.
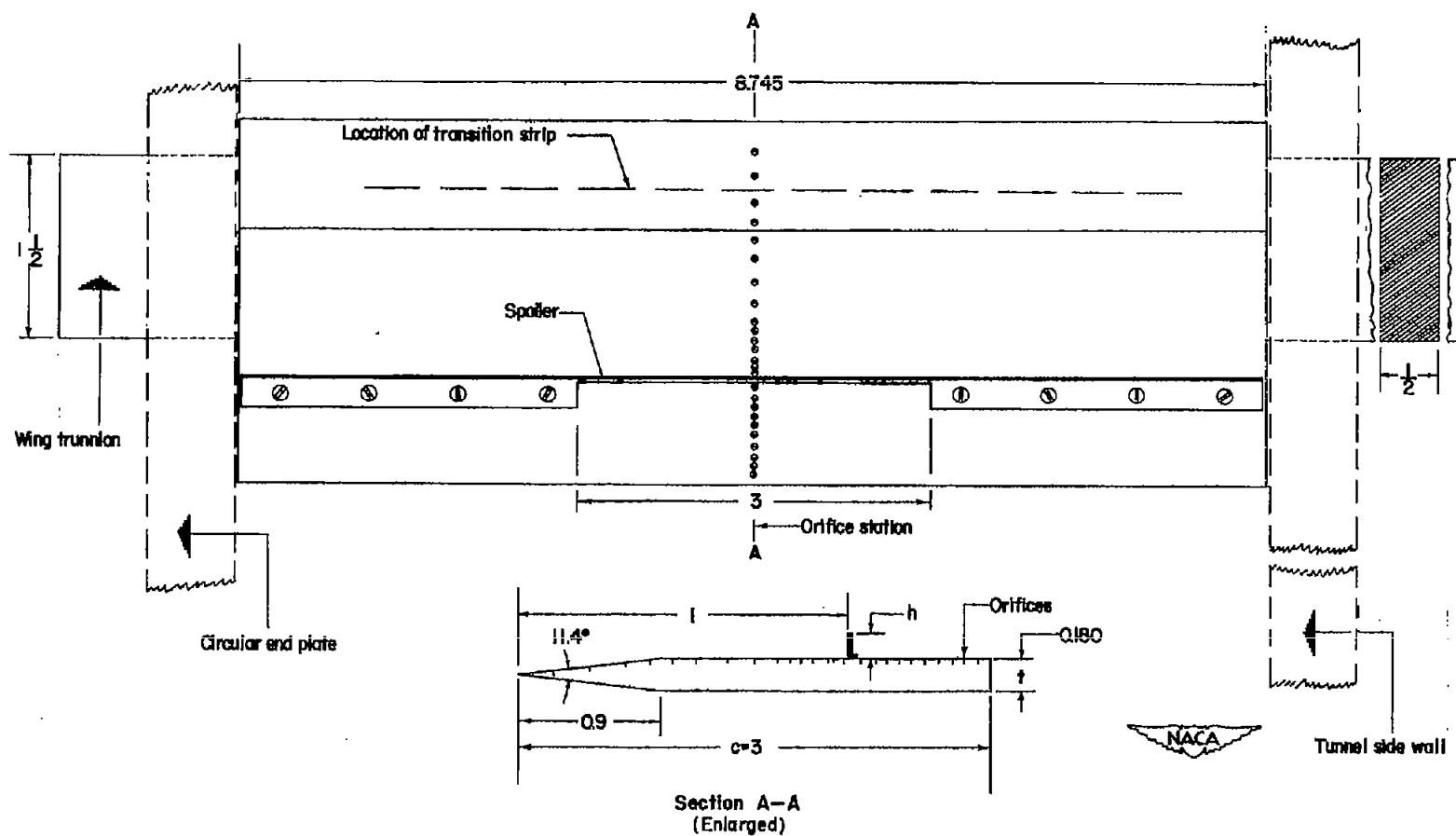
Figure 1.- Dimensional sketch of pressure-distribution model equipped
with spoiler and showing method of mounting model in test section.
All dimensions are in inches.
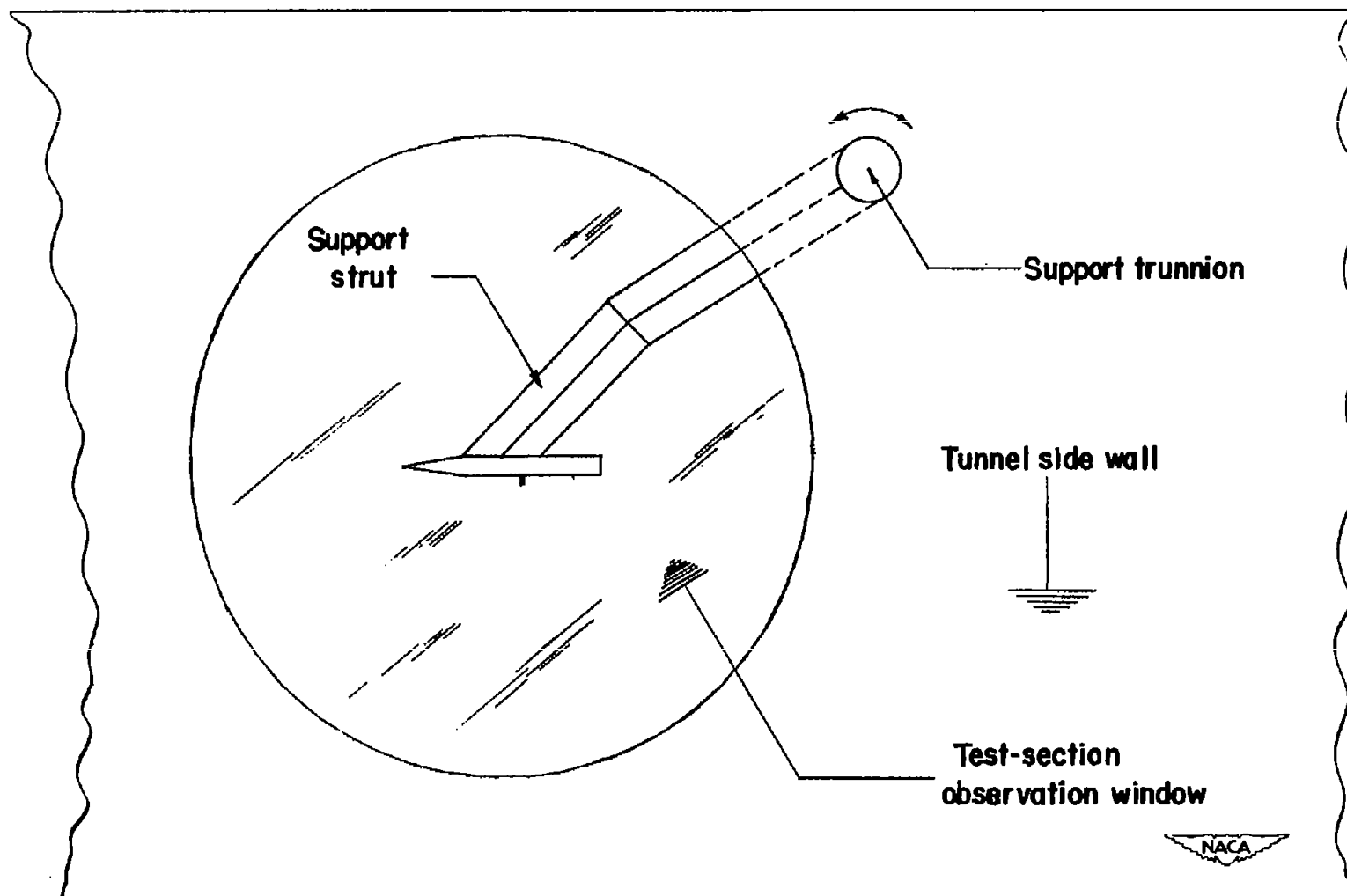
**Figure 2.-** Illustration of method used to mount schlieren model for visual-flow observations.
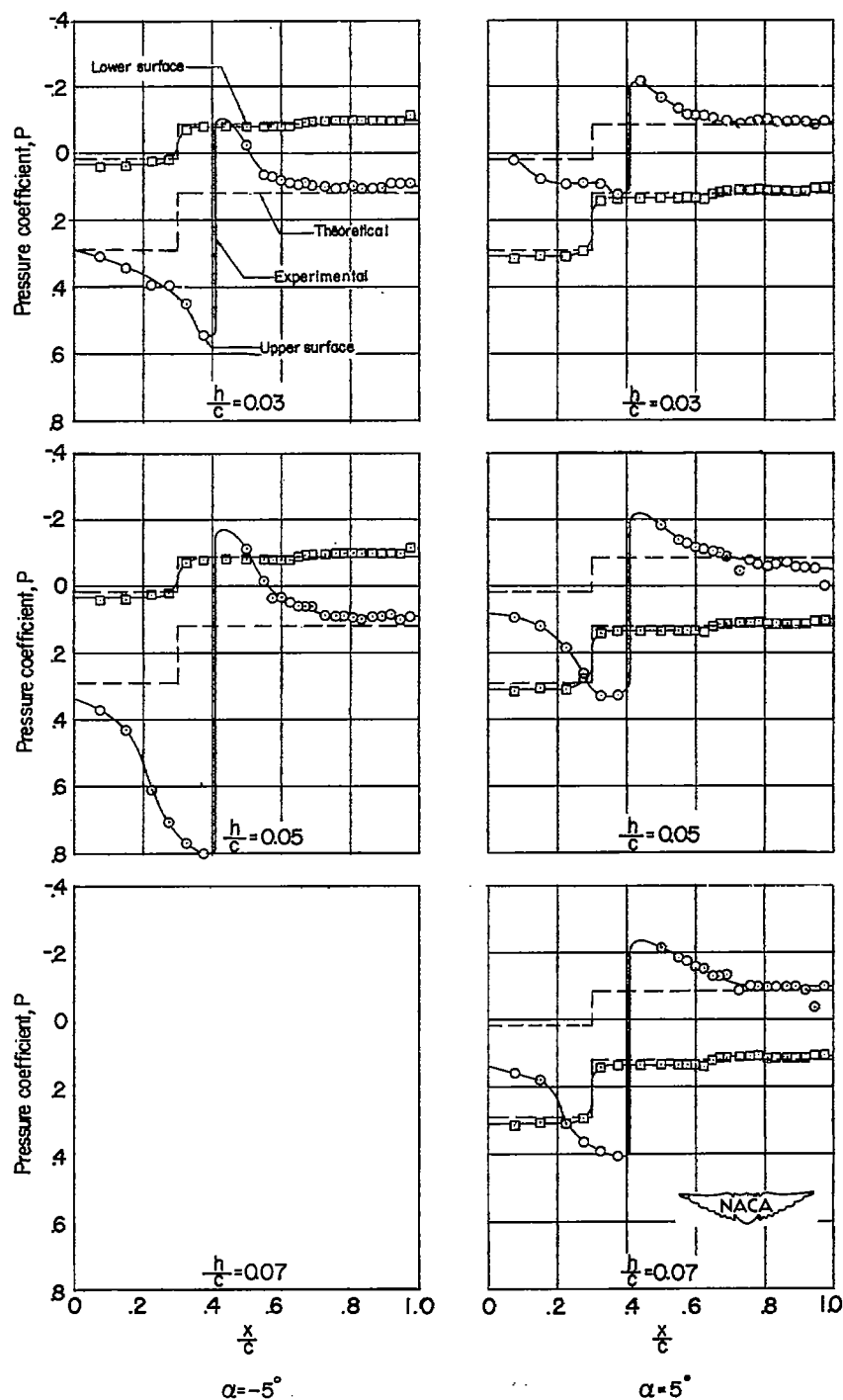
(a) Spoiler location, $l/c$ = 0.41.

Figure 3.- Effect of spoiler height on the pressure distribution over
a 6-percent-thick symmetrical wing. R = 1.03 × 10$^6$.
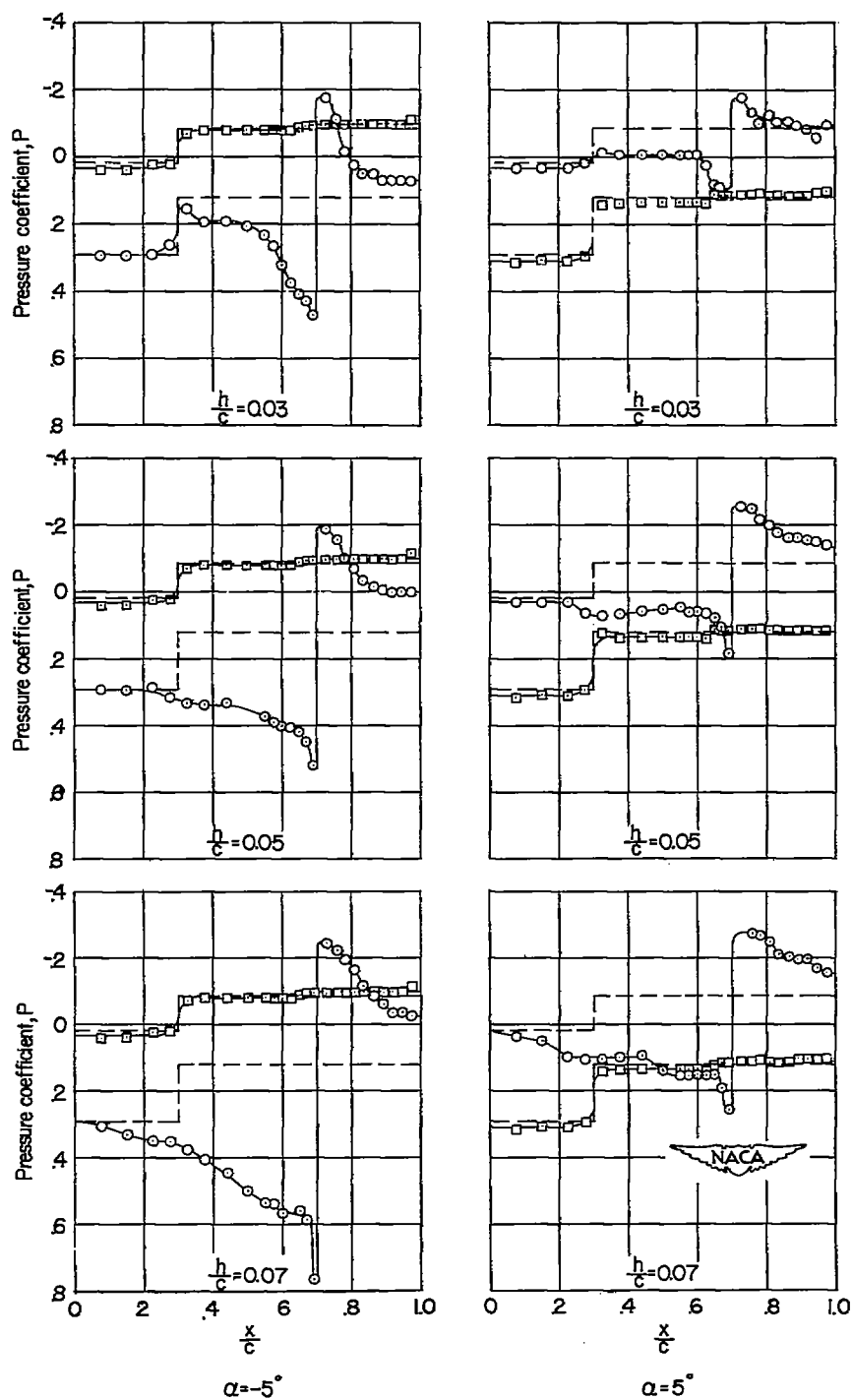
(b) Spoiler location,   $l/c = 0.70$.

Figure 3.- Concluded.
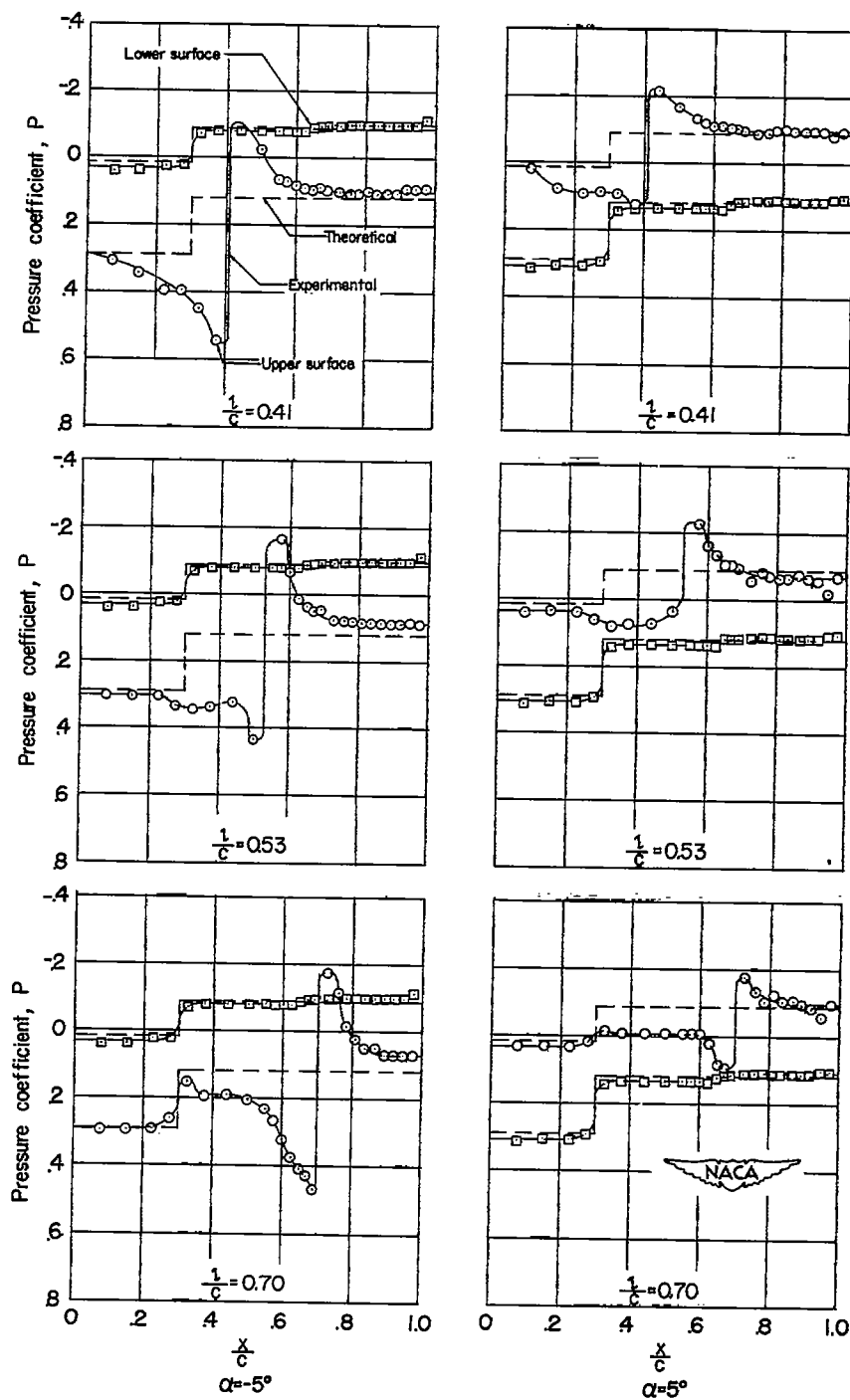
(a) Spoiler height,  h/c = 0.03.

Figure 4.- Effect of spoiler location on the pressure distribution over
a 6-percent-thick symmetric airfoil. R = 1.03 × 10⁶
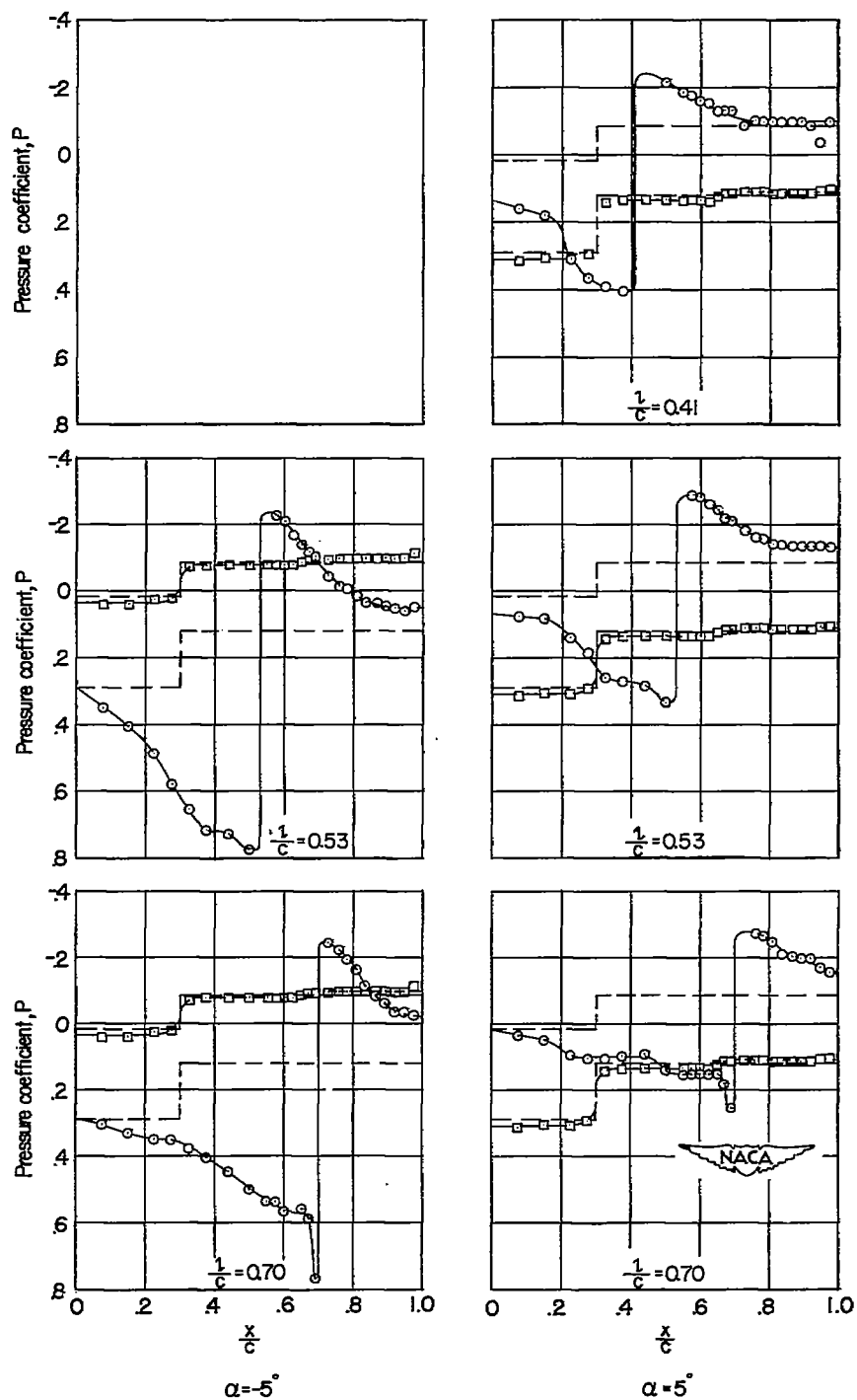
(b) Spoiler height, h/c = 0.07.

Figure 4.- Concluded.
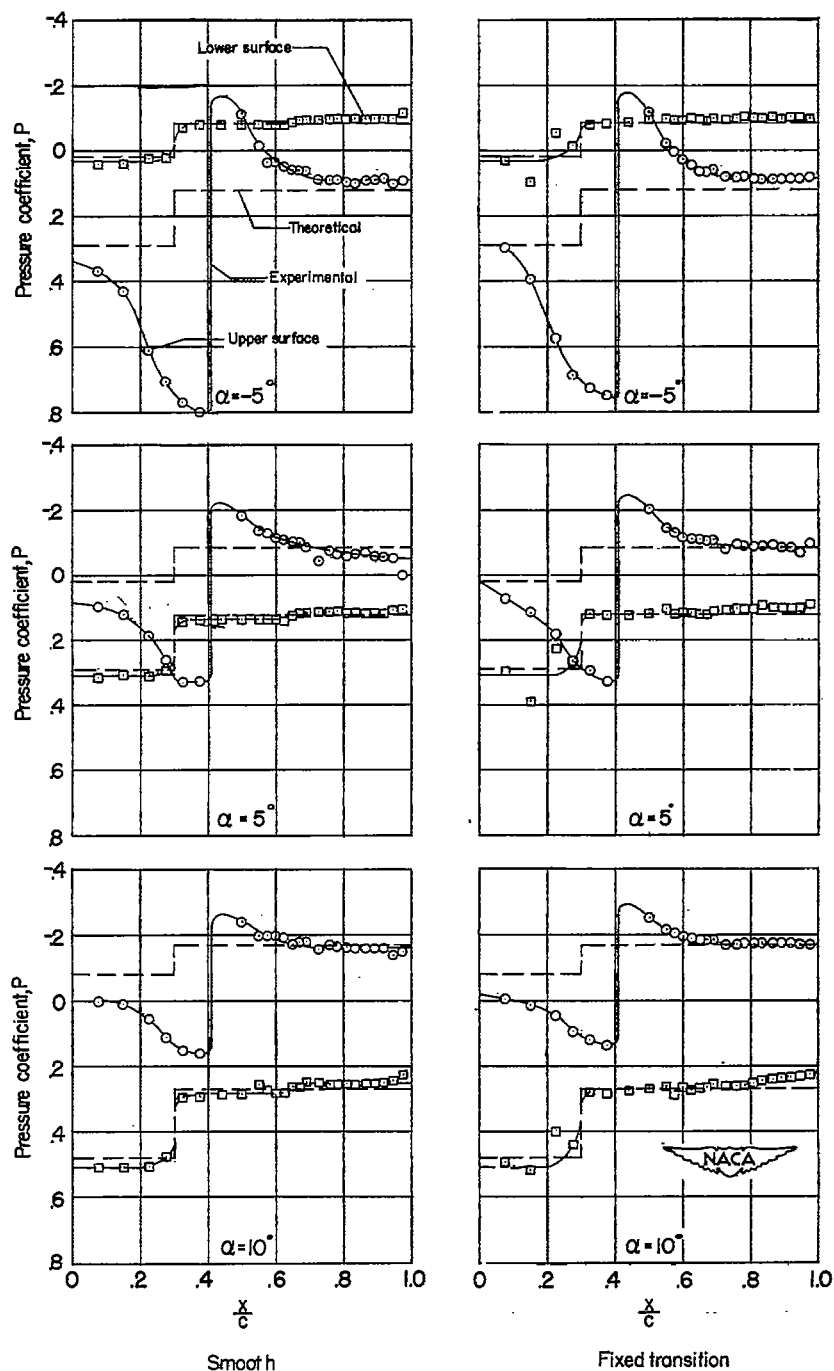
(a) Spoiler location,  $l/c = 0.41$.

Figure 5.- Effect of fixed transition on the pressure distribution over
a 6-percent-thick symmetrical wing.  Spoiler height,  $h/c = 0.05$;
$R = 1.03 \times 10^6$.
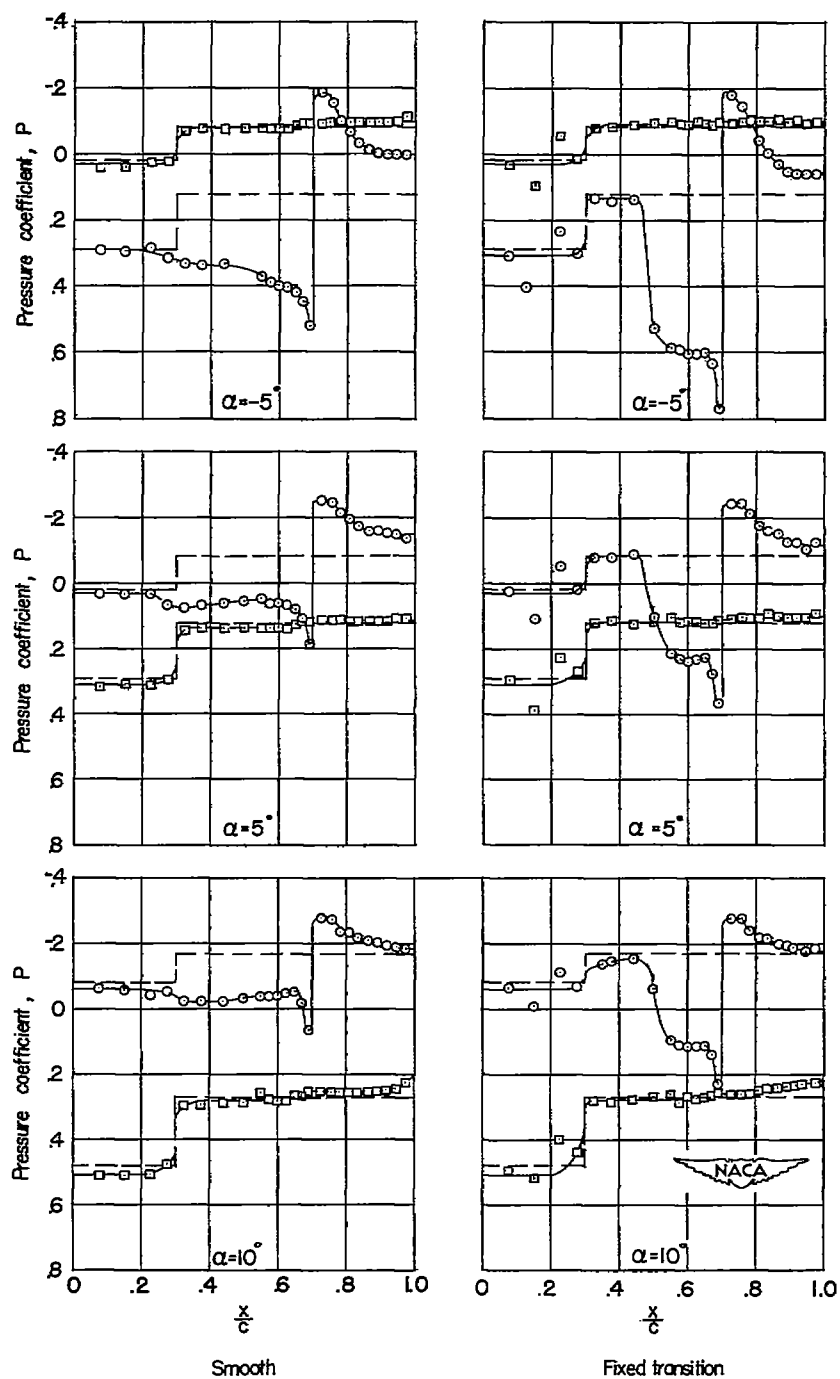
(b) Spoiler location,  $l/c$ = 0.70.

Figure 5.- Concluded.

$\alpha = -5°$

$\alpha = -5°$

$\alpha = -2°$

$\alpha = 0°$

$\alpha = 0°$

$\alpha = 0°$

$\alpha = 5°$

$\alpha = 5°$

$\alpha = 5°$

$h/c = .03$

$h/c = .05$

$h/c = .07$
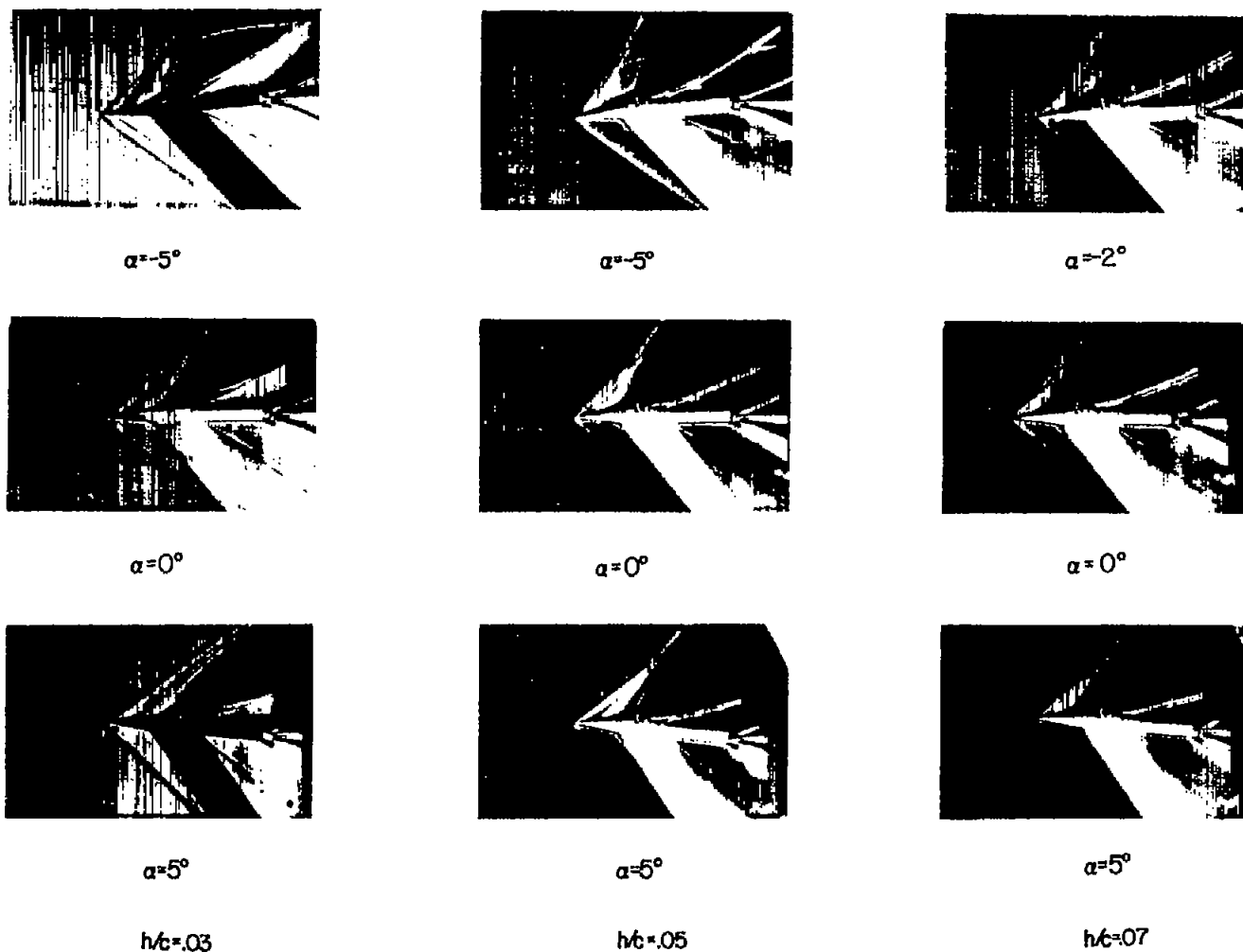
(a) Spoiler location, $l/c = 0.41$.

L-77900

Figure 6.- Schlieren photographs of flow about a 6-percent-thick symmetrical wing equipped with spoilers of various heights. $R = 1.03 \times 10^6$.

$\alpha=-5°$    $\alpha=-5°$

$\alpha=0°$    $\alpha=0°$

$\alpha=5°$    $\alpha=5°$

h/c=.03    h/c=.05    h/c=.07
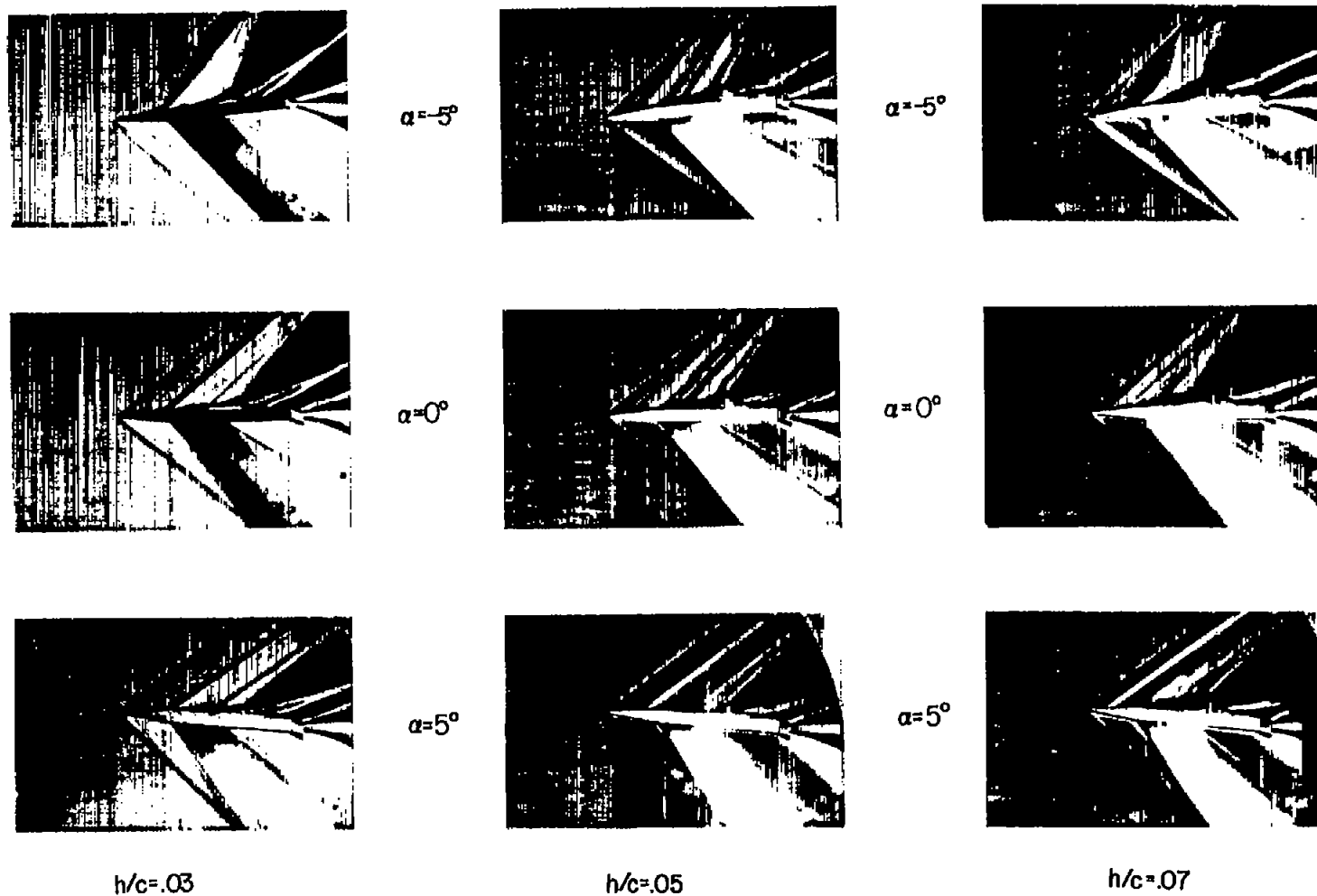
(b) Spoiler location, $l/c = 0.70$.

Figure 6.- Concluded.

L-77901

$\alpha = -5°$

$\alpha = -2°$

$\alpha = 0°$

$\alpha = 2°$

$\alpha = 5°$

$\alpha = 10°$

L-77902

$x/c = .41$

$x/c = .70$
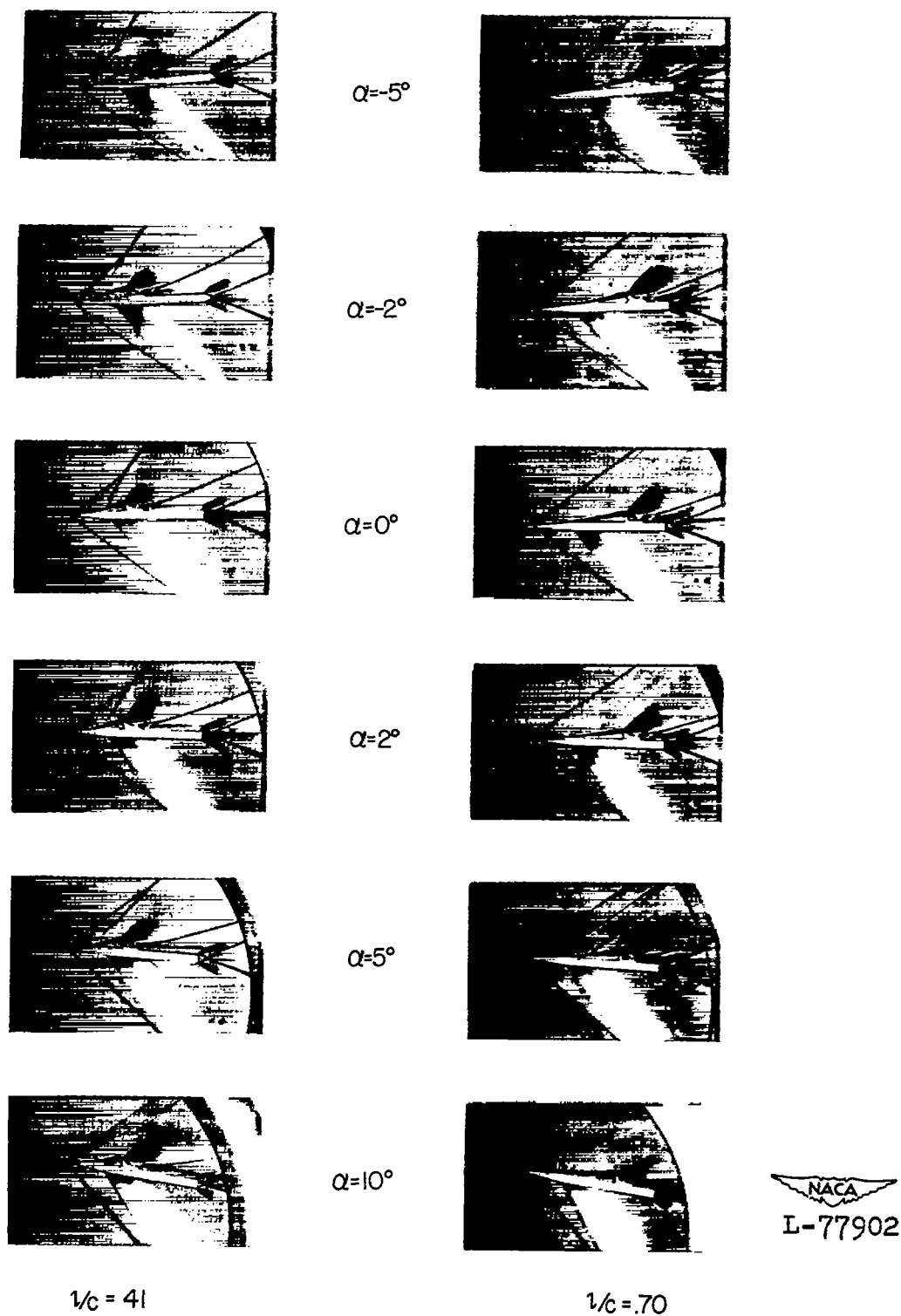
Figure 7.- Shadowgraphs of flow about a 6-percent-thick symmetrical wing equipped with spoiler. Spoiler height, $h/c = 0.05$; $R = 1.03 \times 10^6$.

$\alpha = -5°$

$\alpha = -10°$

$\alpha = 0°$

$\alpha = 0°$

$\alpha = 5°$

$\alpha = 5°$

$1/c = .41$

$1/c = .53$

$1/c = .70$
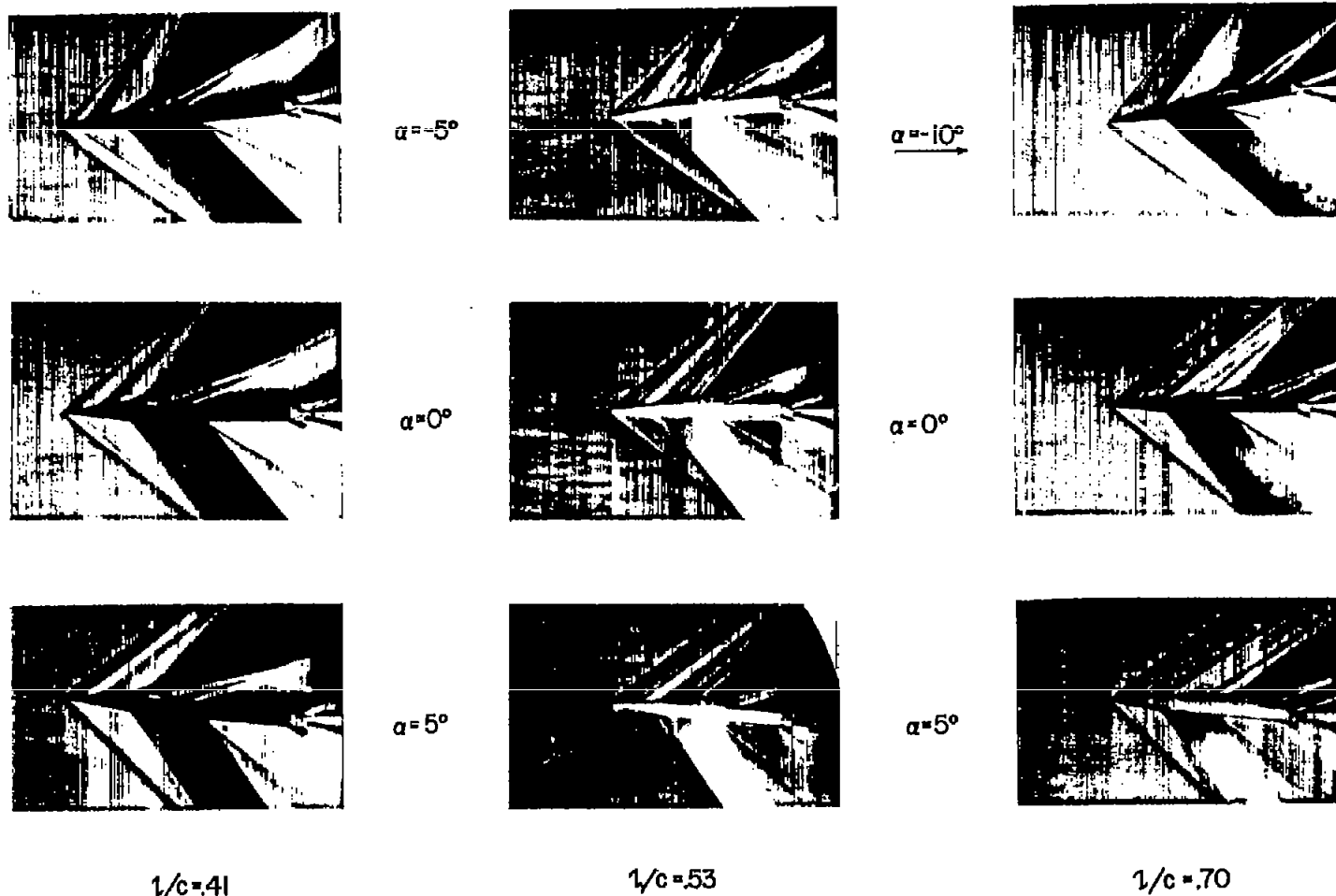
(a) Spoiler height, $h/c = 0.03$.

L-77903

Figure 8.- Schlieren photographs of flow about a 6-percent-thick symmetrical wing equipped with spoilers at various chordwise locations. $R = 1.03 \times 10^6$.

$\alpha = -2°$

$\alpha = -5°$

$\alpha = 0°$

$\alpha = 0°$

$\alpha = 5°$

$\alpha = 5°$

$l/c = .53$

$l/c = .70$

$l/c = .41$

(b) Spoiler height,  $h/c = 0.07$.

L-77904

Figure 8.- Concluded.

$\alpha = -5°$

$\alpha = -2°$
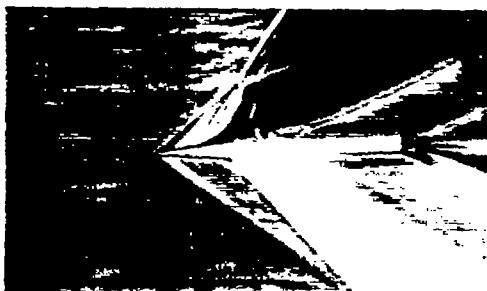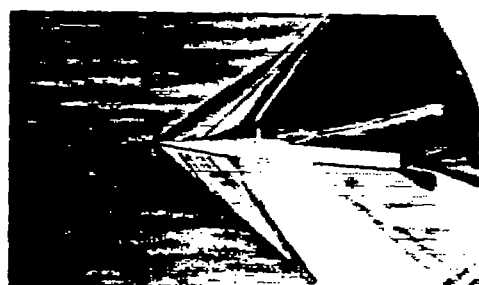
Smooth          $\alpha = 5°$          Fixed transition

(a) Spoiler location, $l/c = 0.41$.

L-77905

Figure 9.- Schlieren photographs of flow about a 6-percent-thick
symmetrical wing equipped with a spoiler with and without fixed
transition. Spoiler height, $h/c = 0.05$; $R = 1.87 \times 10^6$.

$\alpha = -5°$



$\alpha = -2°$
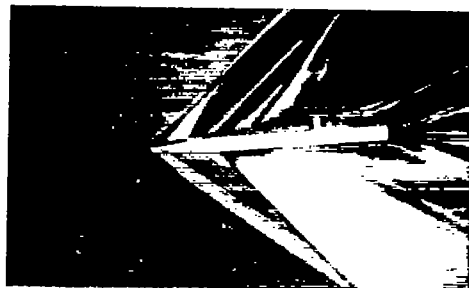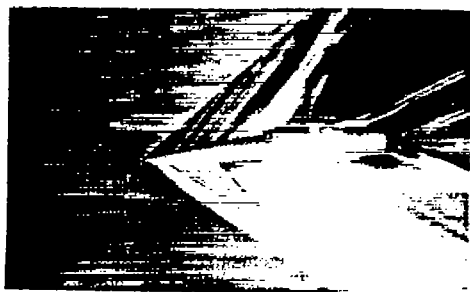


Smooth               $\alpha = 5°$               Fixed transition

(b) Spoiler location,  $l/c = 0.70$.

Figure 9.- Concluded.
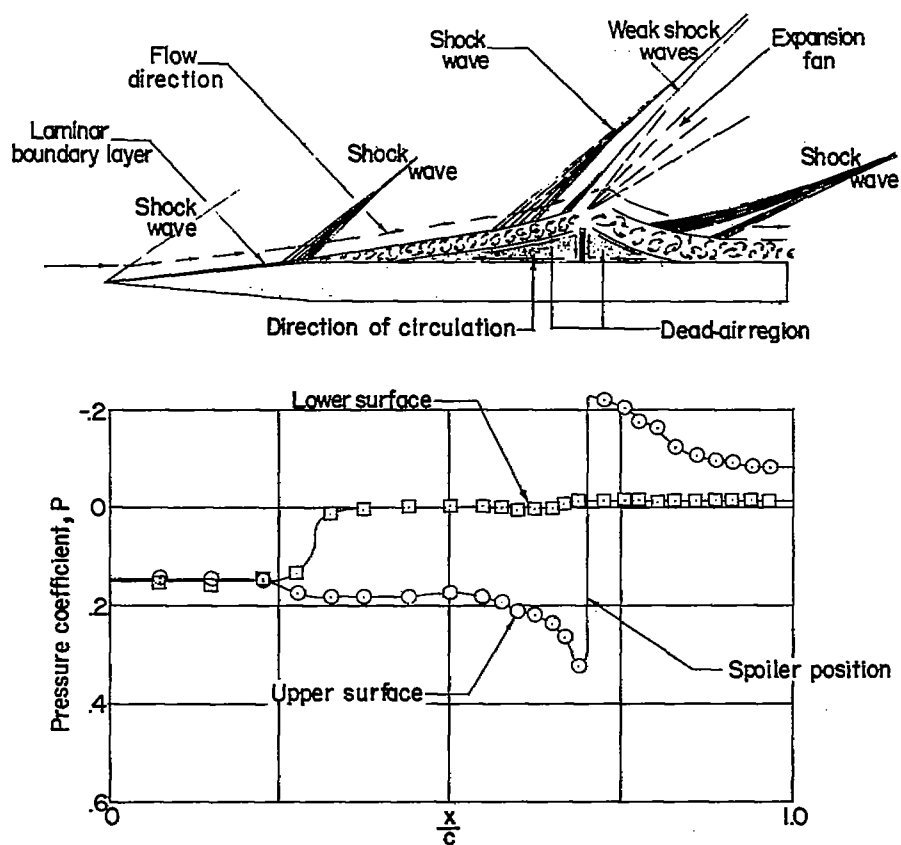
L-77906

(a) Laminar boundary layer.          L-77907

Figure 10.- Effect of varying the boundary layer on the flow over a
6-percent-thick symmetrical wing equipped with a spoiler having a
height of 0.05 chord.  $\alpha = 0^\circ$; $R = 1.03 \times 10^6$.
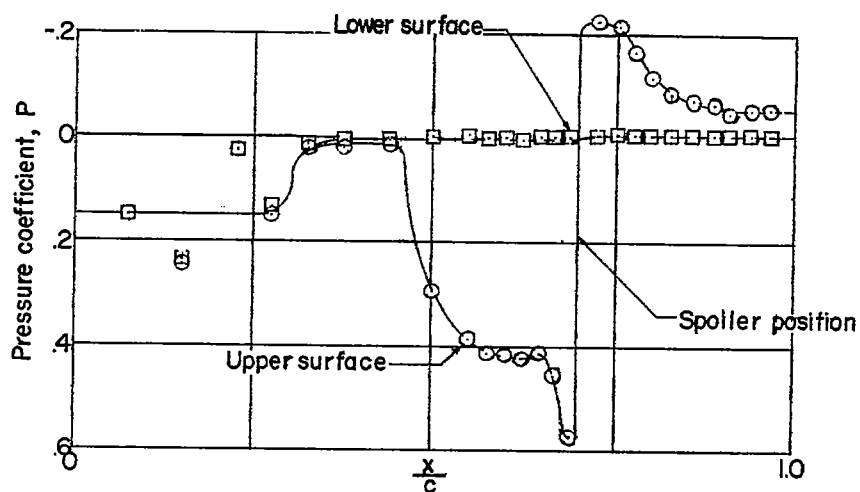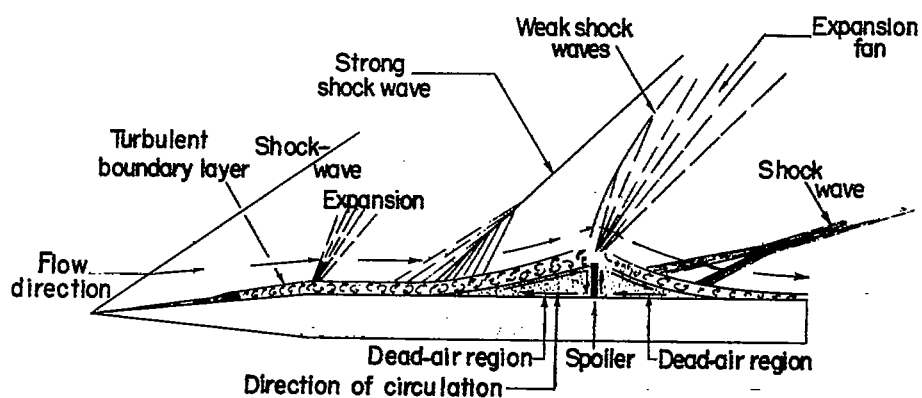
(b) Turbulent boundary layer.

Figure 10.- Concluded.
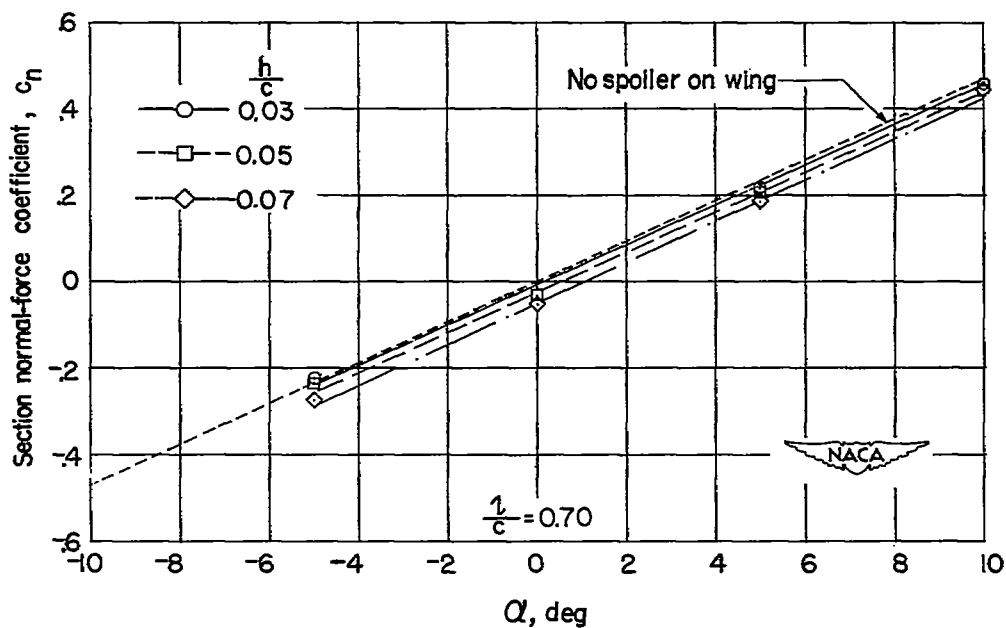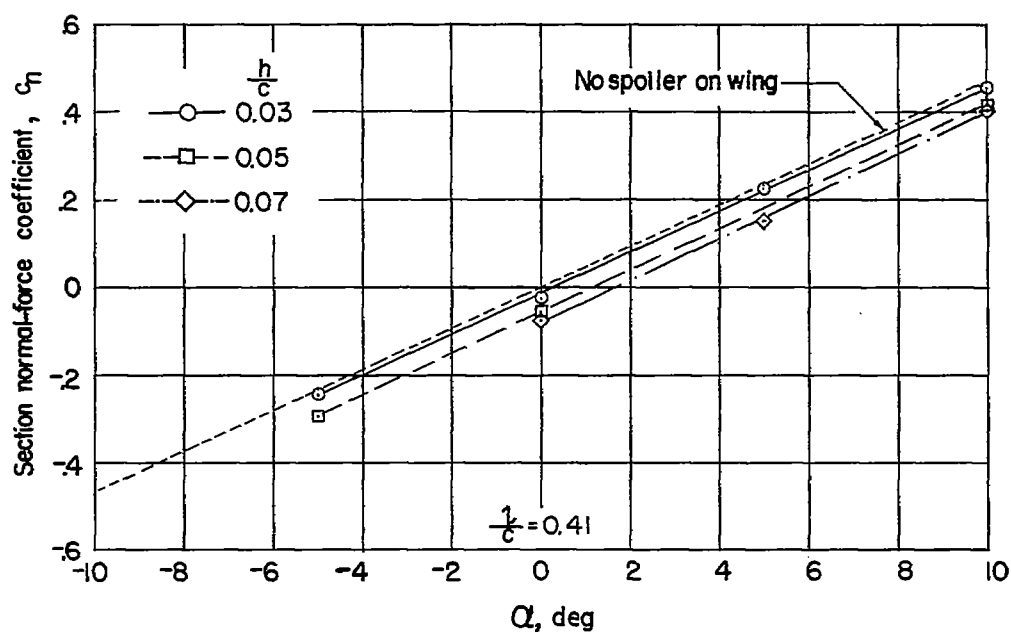
(a) $c_n$ against $\alpha$.

Figure 11.- Effect of spoiler height on the section normal-force
    coefficients of a 6-percent-thick symmetrical wing.  $R = 1.03 \times 10^6$.
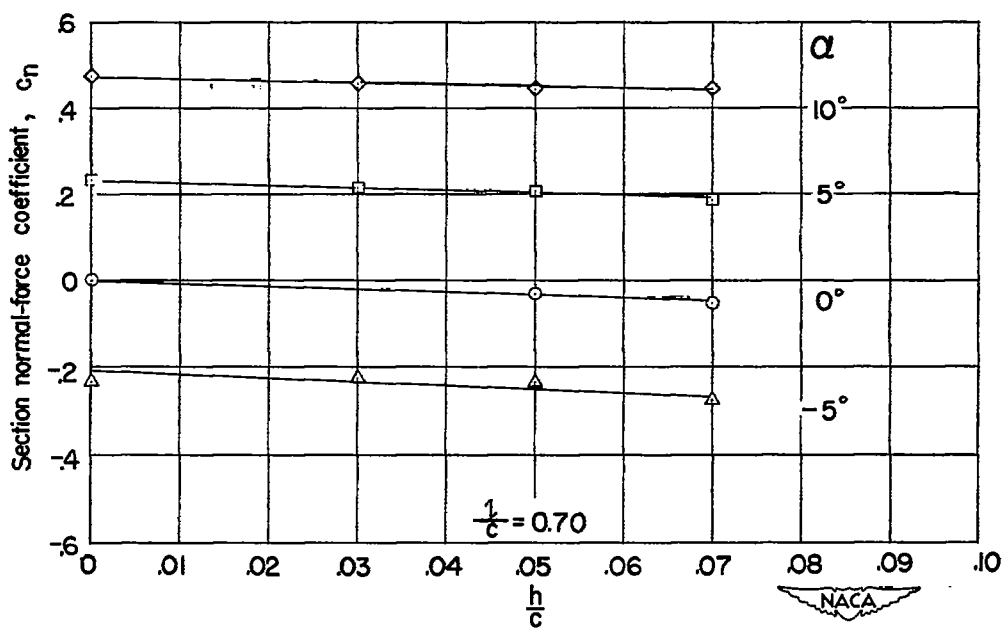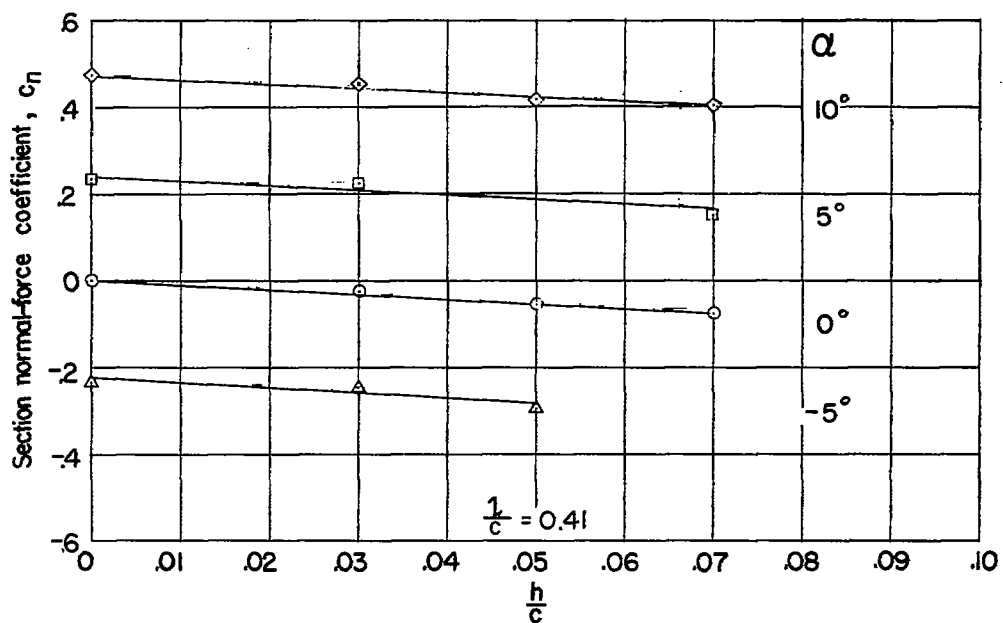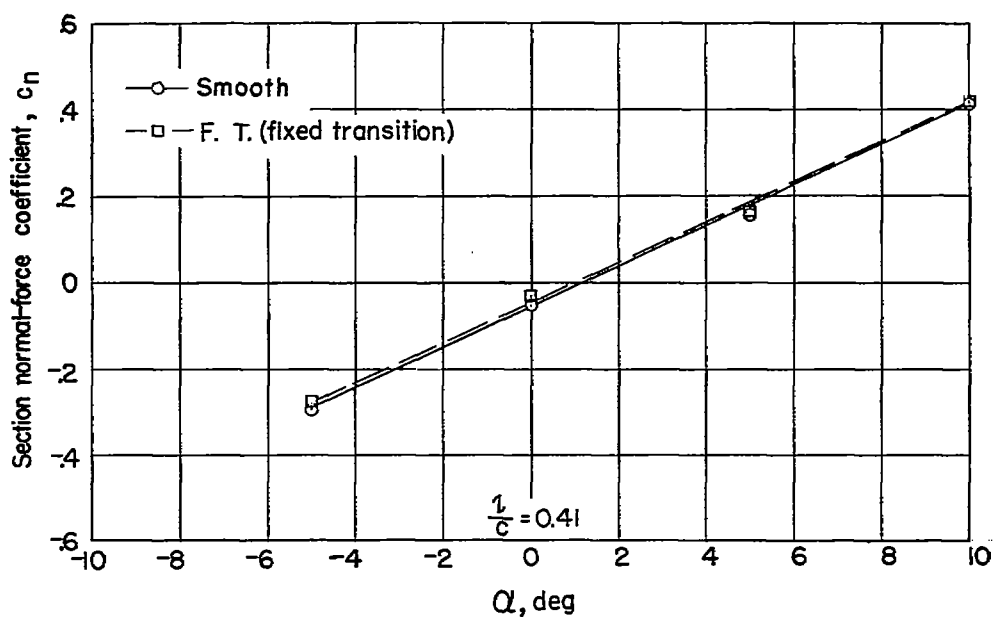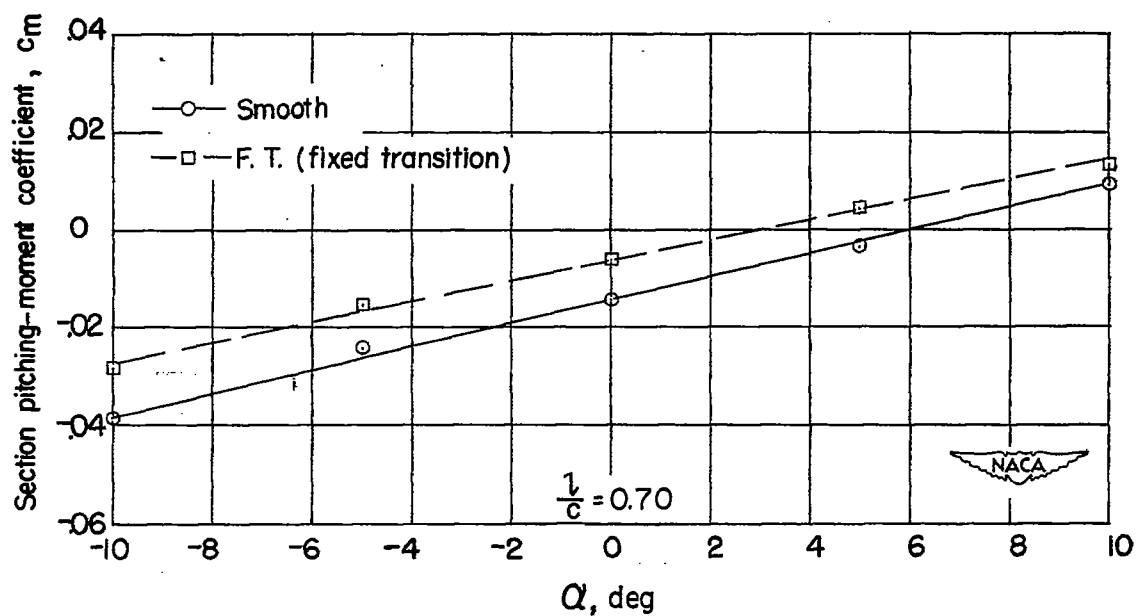
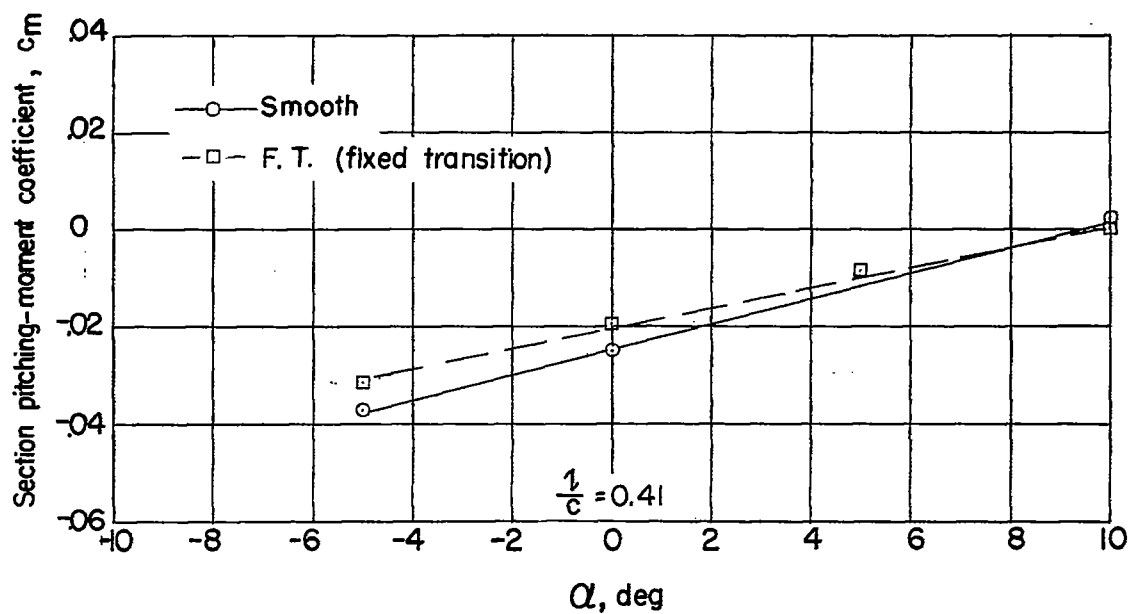(b)  $c_n$  against  h/c.

Figure 11.- Concluded.
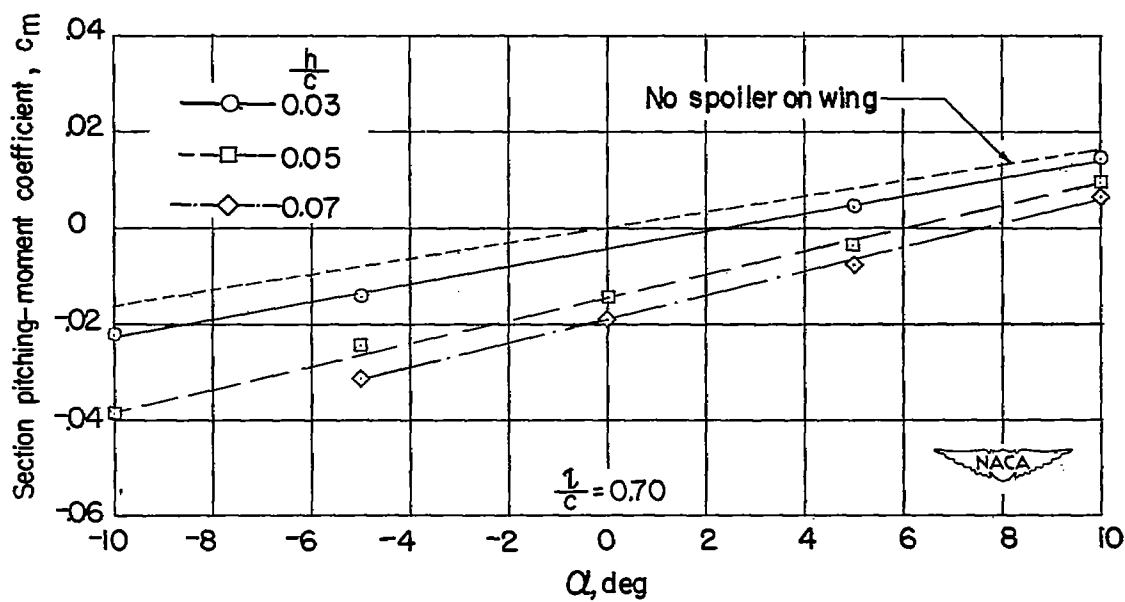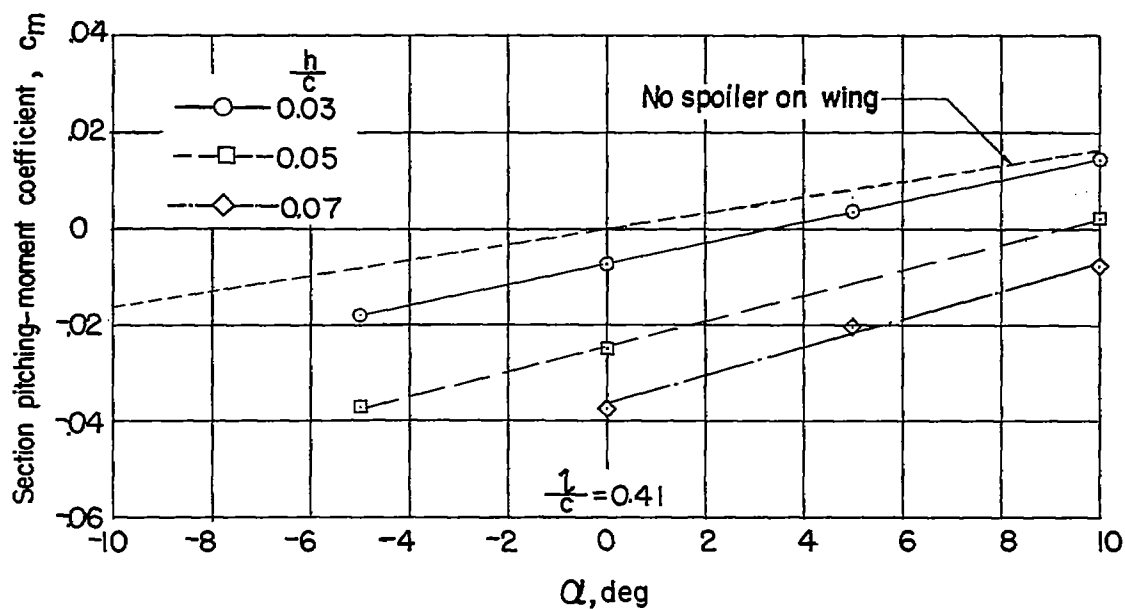
(a) $c_m$ against $\alpha$.

Figure 12.- Effect of spoiler height on the section pitching-moment
coefficients of a 6-percent-thick symmetrical wing.  R = 1.03 × 10^{6}.
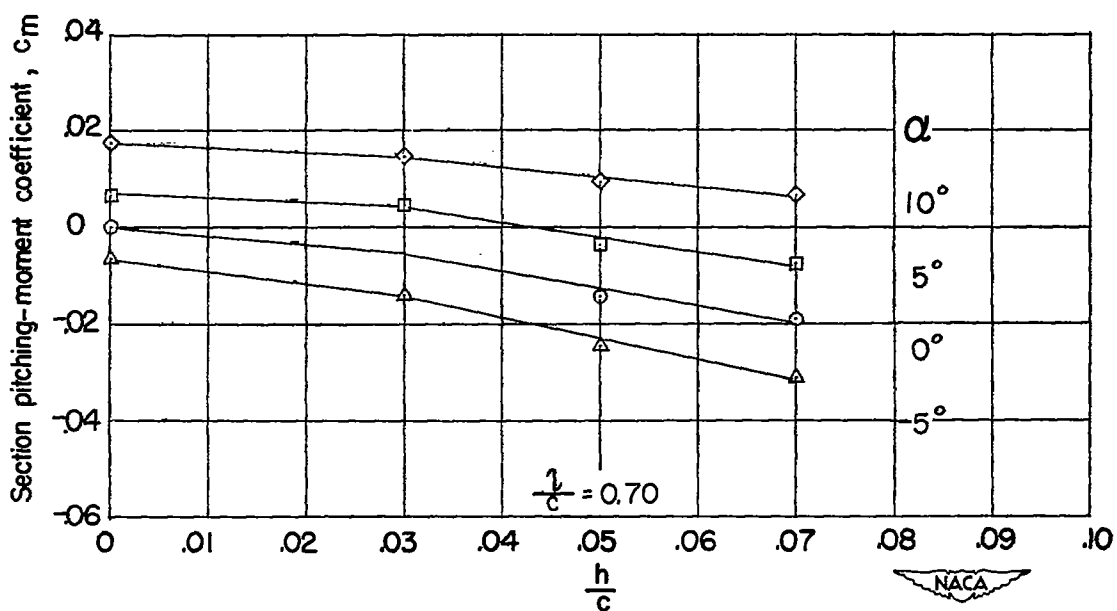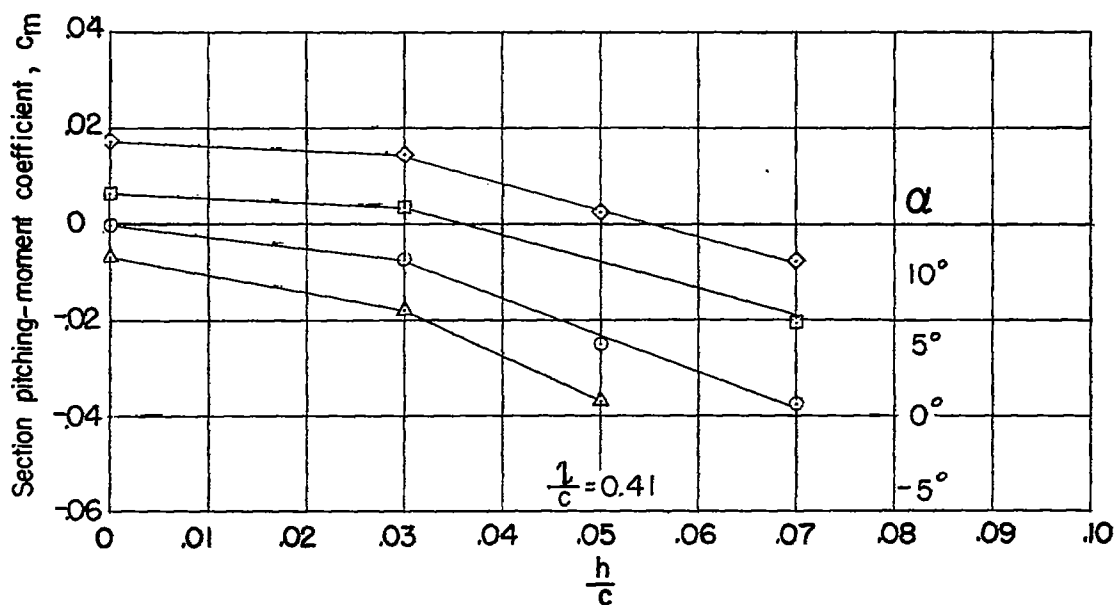
(b)  $c_m$  against  h/c.

Figure 12.- Concluded.
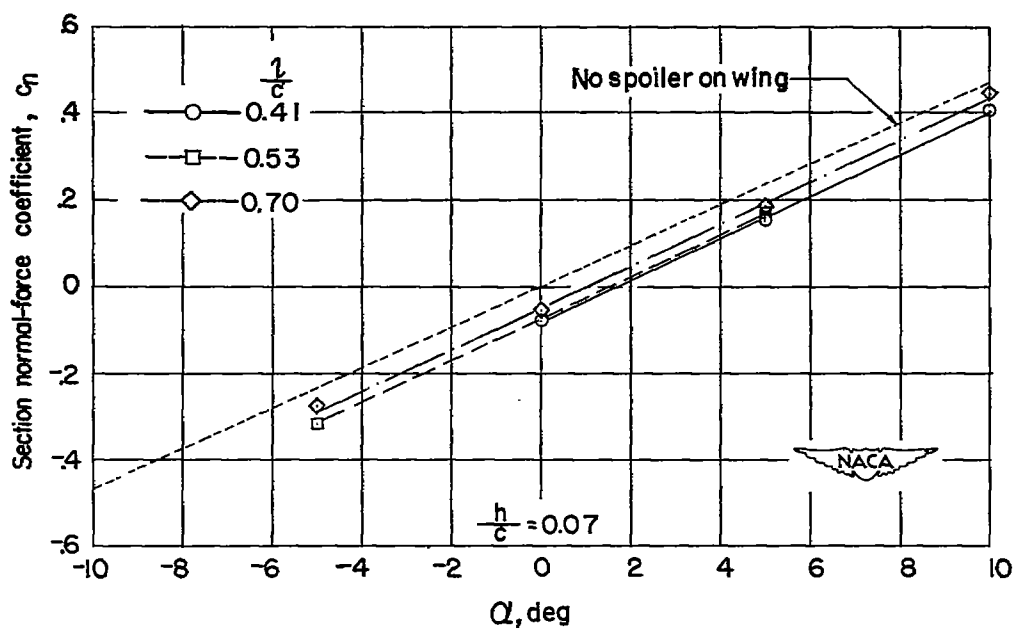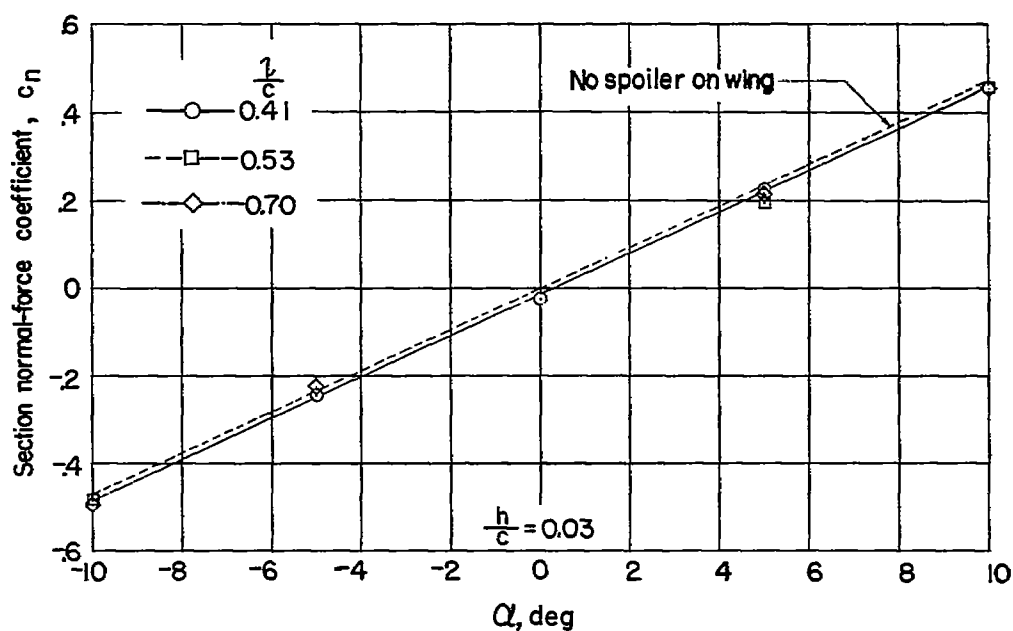
(a)  $c_n$  against  $\alpha$.

Figure 13.- Effect of spoiler location on the section normal-force
    coefficients of a 6-percent-thick symmetrical wing.  R = 1.03 × 10^{6}.
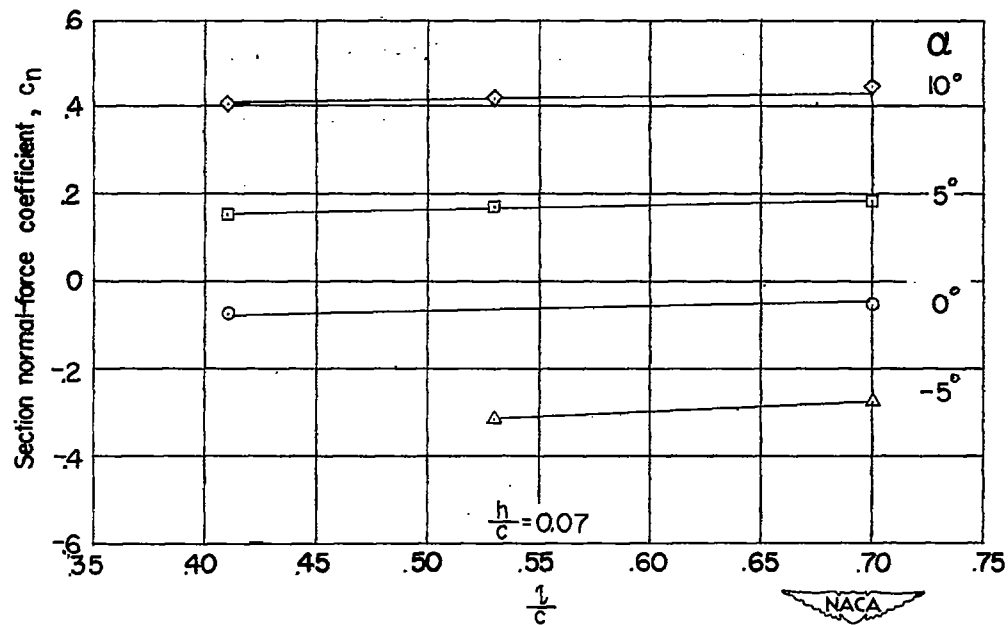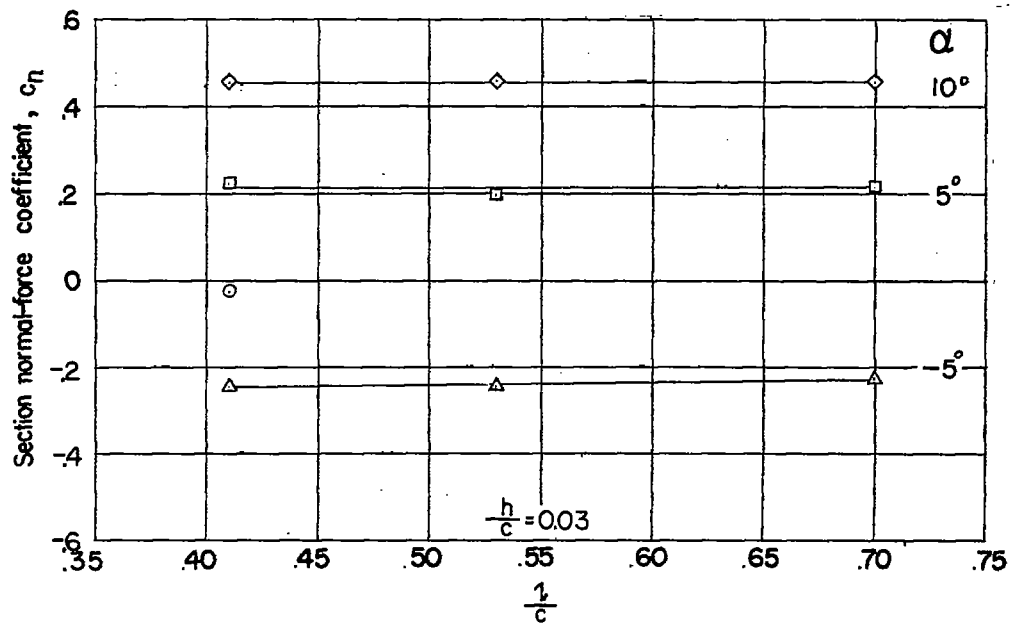
(b)  $c_n$  against  $l/c$.

Figure 13.- Concluded.
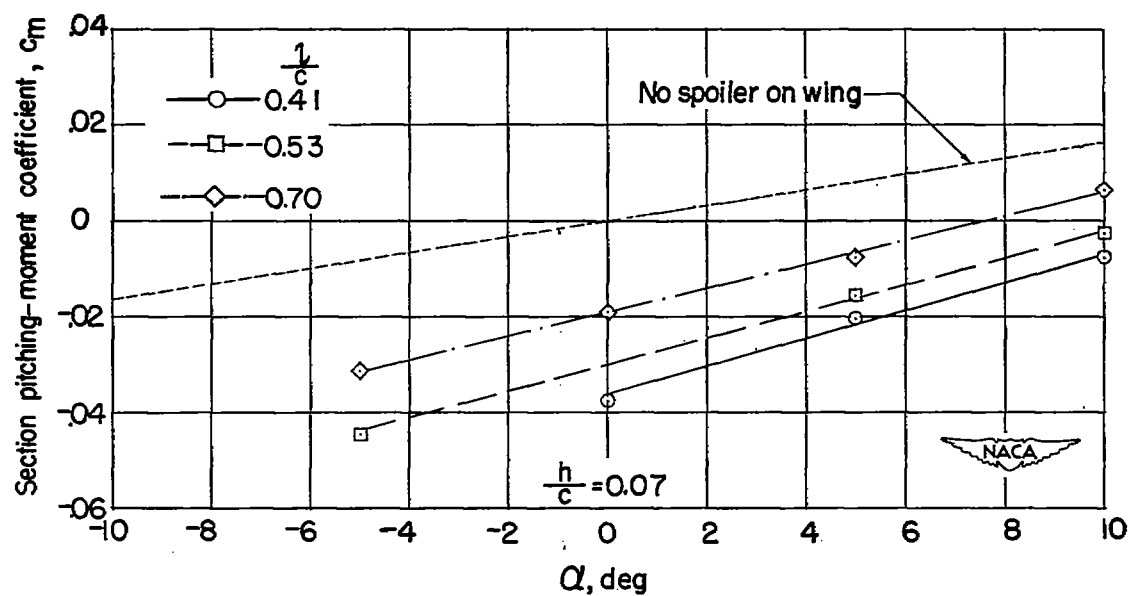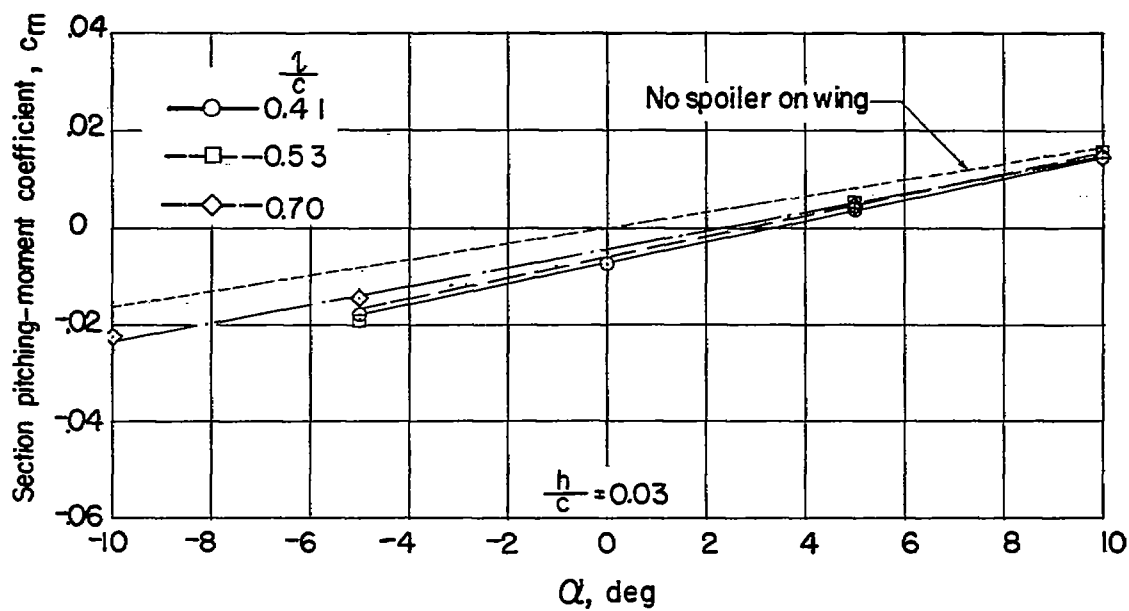
(a) $c_m$ against $\alpha$.

Figure 14.- Effect of spoiler location on the section pitching-moment coefficients of a 6-percent-thick symmetrical wing. $R = 1.03 \times 10^6$.
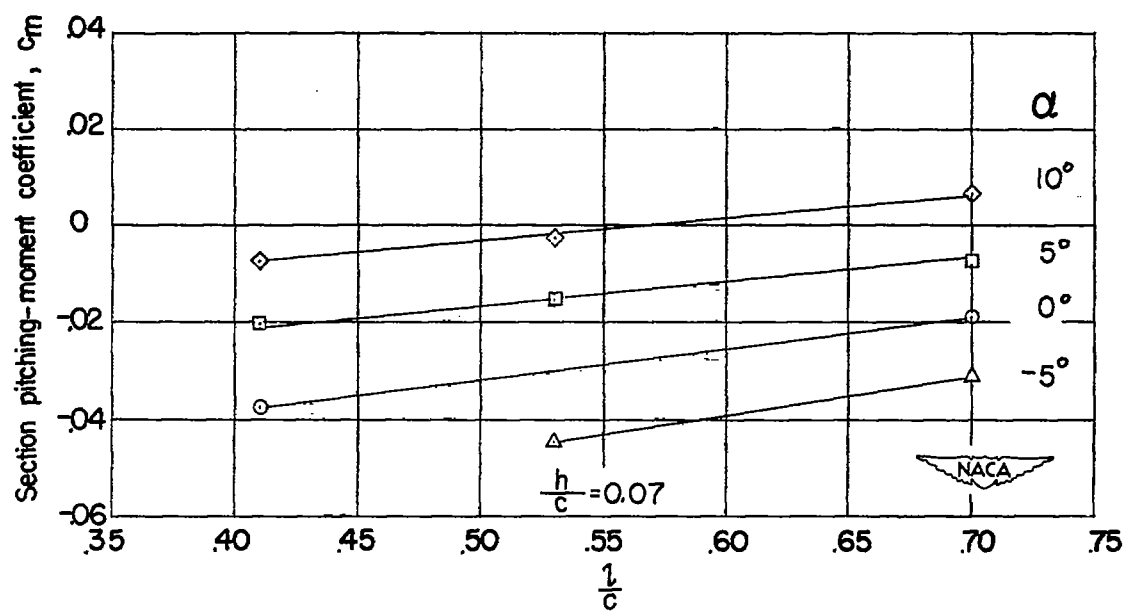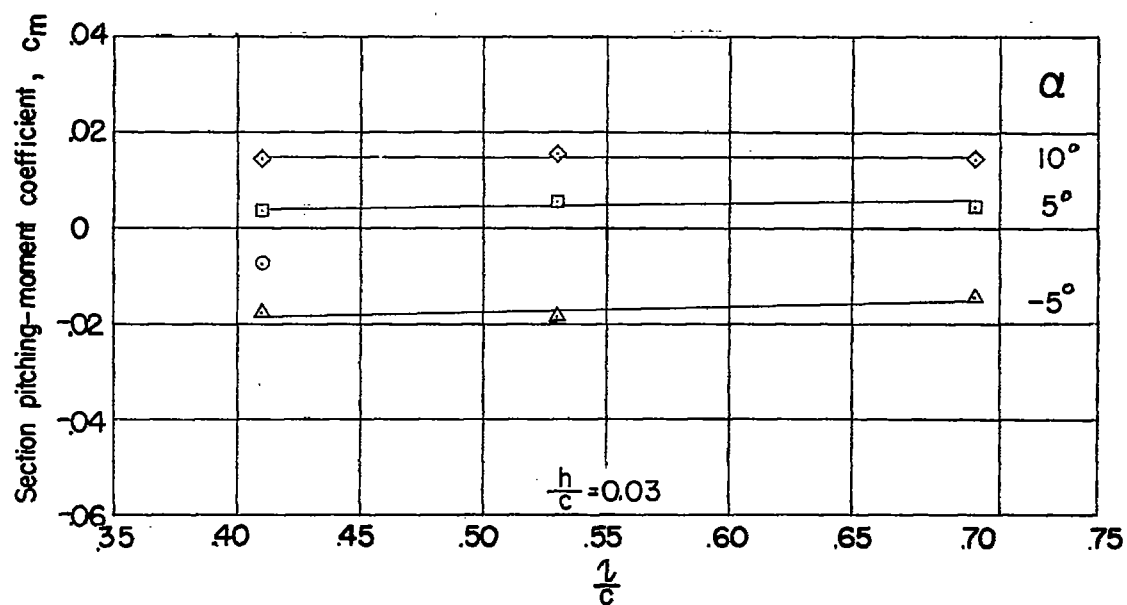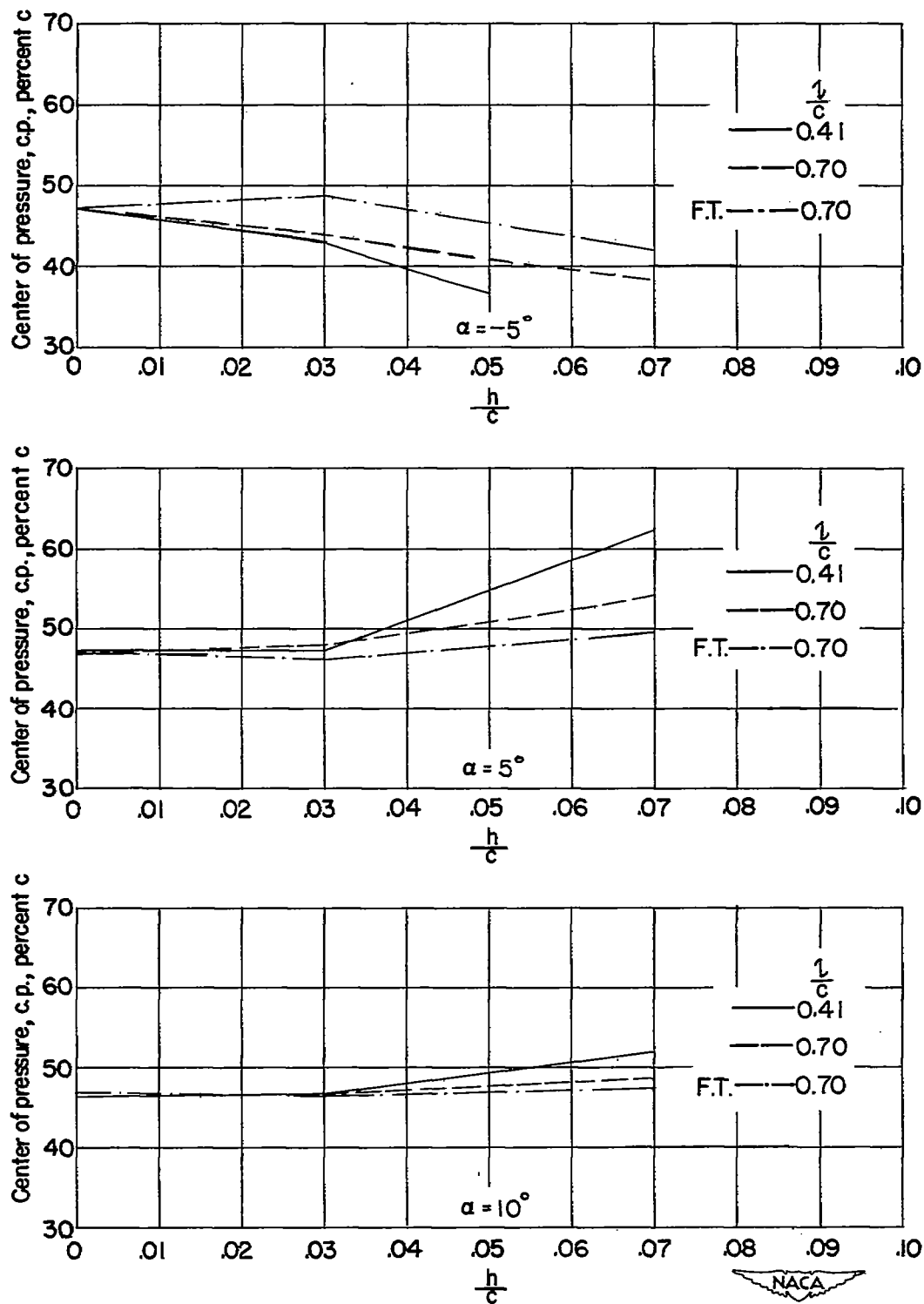
(b) $c_m$ against $l/c$.

Figure 14.- Concluded.
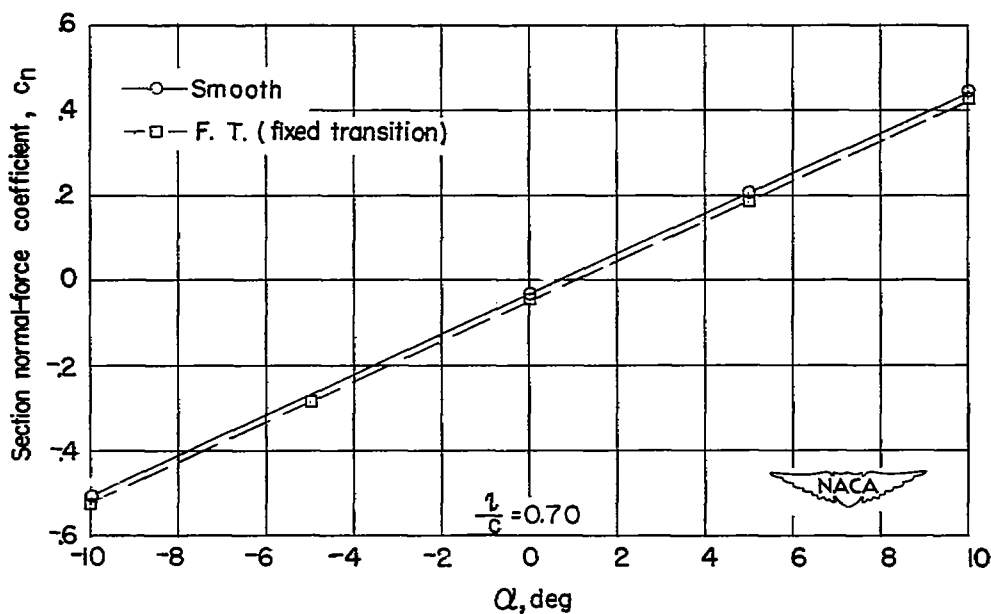
(a) $c_n$ against $\alpha$.

Figure 15.- Effect of fixed transition on the section normal-force and pitching-moment coefficients of a 6-percent-thick symmetrical wing. $h/c = 0.05$; $R = 1.03 \times 10^6$.

(b)  $c_m$  against  $\alpha$.

Figure 15.- Concluded.

Figure 16.- Variation of wing center of pressure with spoiler height.
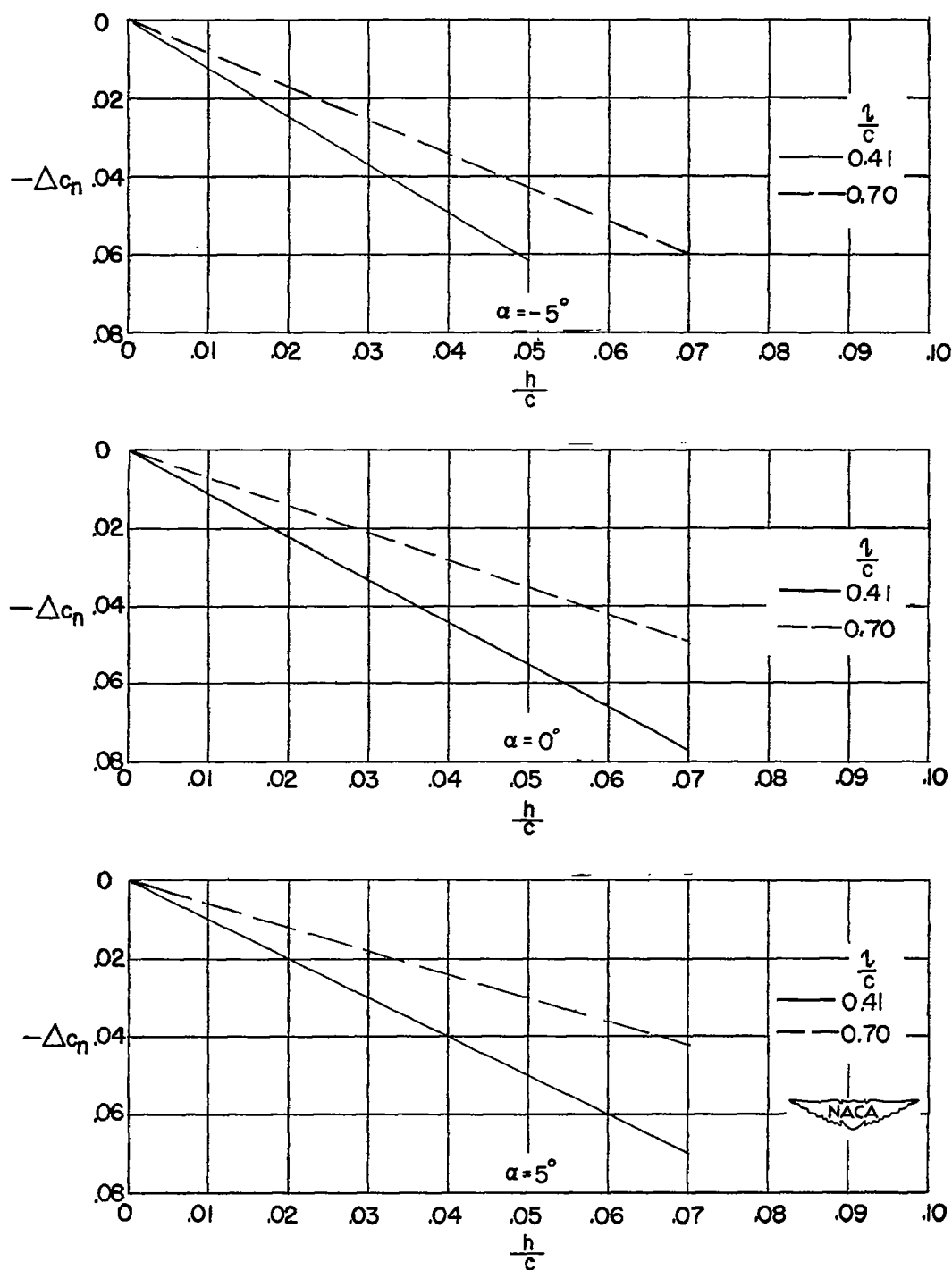$R = 1.03 \times 10^6$.

(a)  $\Delta c_n$  against  h/c.

Figure 17.- Effect of spoiler height on the incremental section normal-
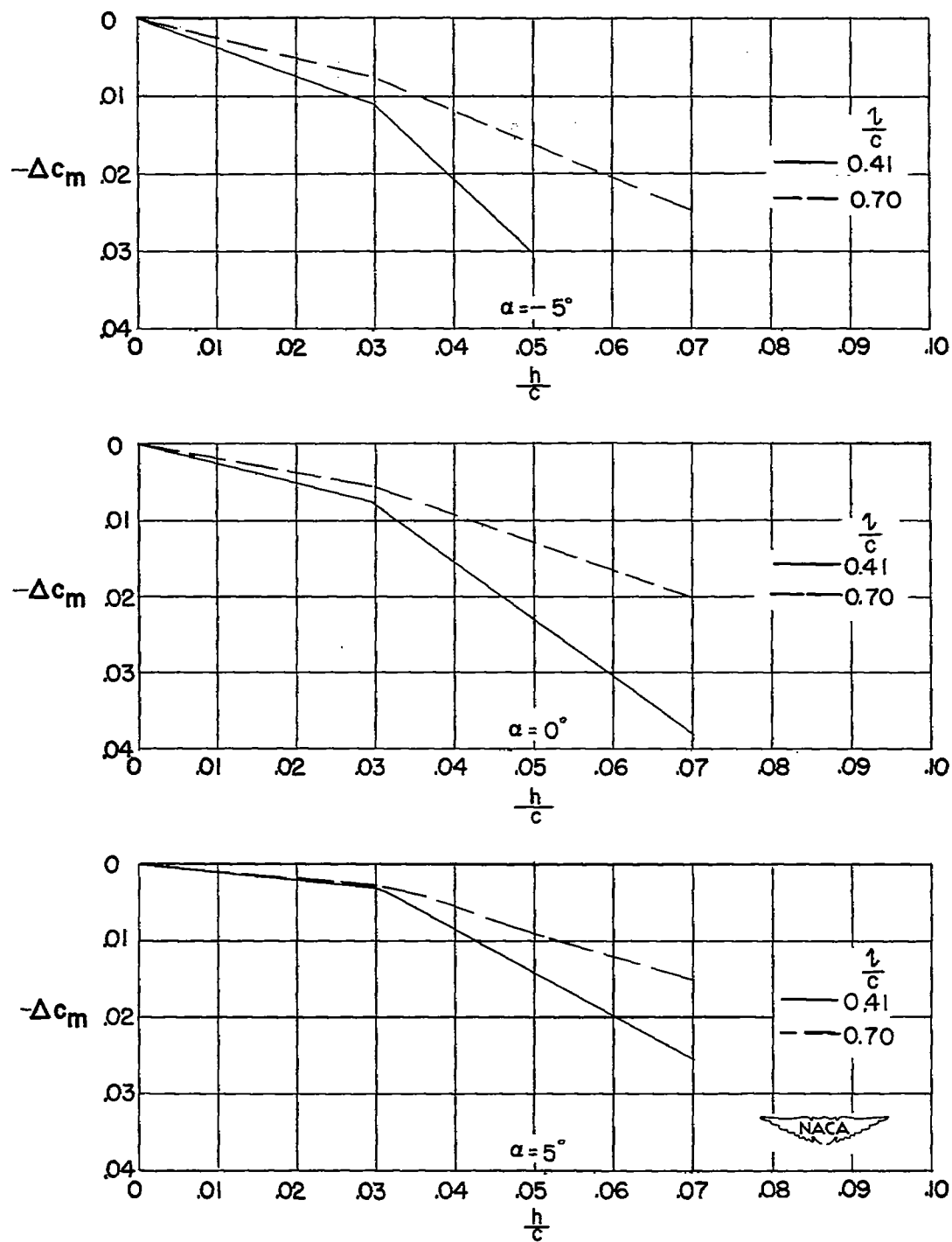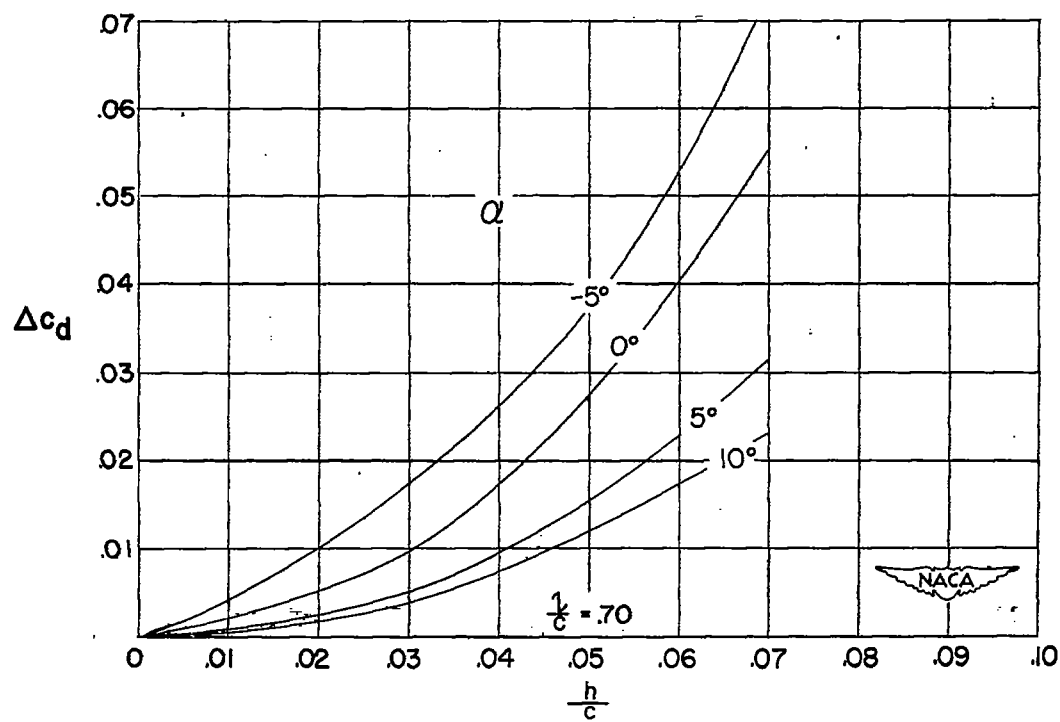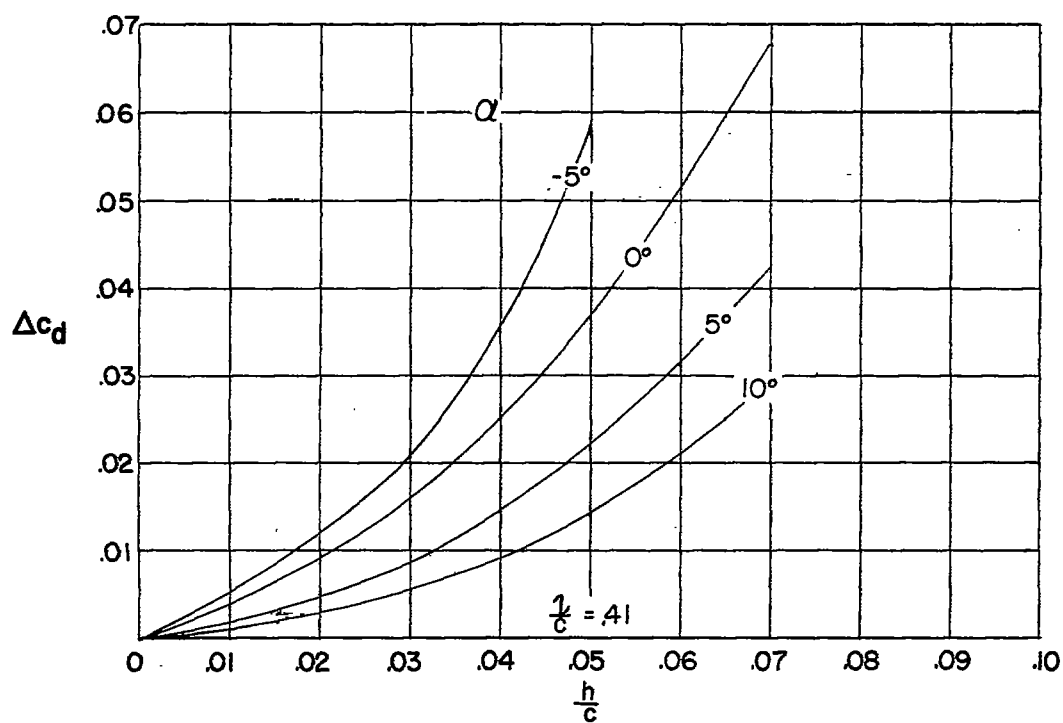force, pitching-moment, and pressure-drag coefficients.  R = 1.03 × 10^{6}.

(b) $\Delta c_m$ against h/c.

Figure 17.- Continued.

(c) $\Delta c_d$ against h/c.

Figure 17.- Concluded.

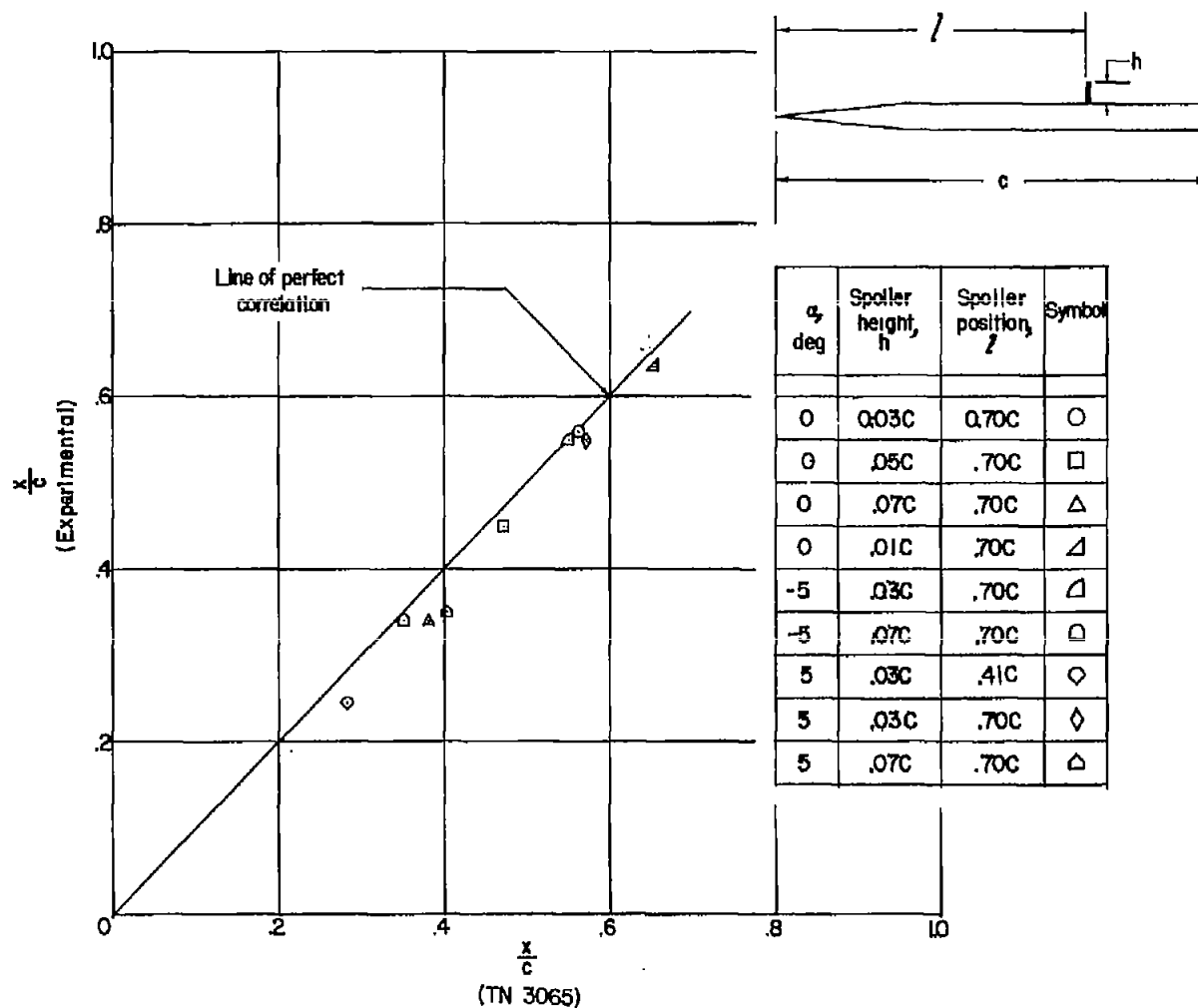| a, deg | Spoiler height, h | Spoiler position, l | Symbol |
|--------|-------------------|---------------------|--------|
| 0 | 0.03C | 0.70C | ○ |
| 0 | .05C | .70C | □ |
| 0 | .07C | .70C | △ |
| 0 | .01C | .70C | ◿ |
| -5 | .03C | .70C | ◹ |
| -5 | .07C | .70C | ◺ |
| 5 | .03C | .41C | ◇ |
| 5 | .03C | .70C | ◊ |
| 5 | .07C | .70C | △ |

Figure 18.- Comparison between theory and experiment of the chordwise point of flow separation from the surface of a wing equipped with spoilers of various heights located at two chordwise positions. Turbulent boundary layer.

(a) Schlieren photograph.
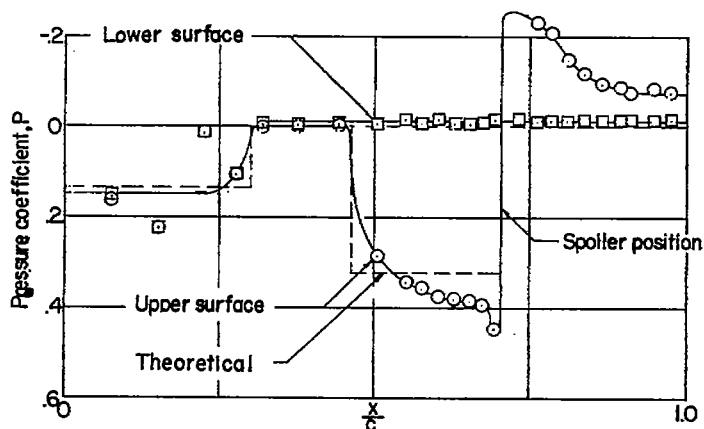


(b) Experimental pressure distribution.
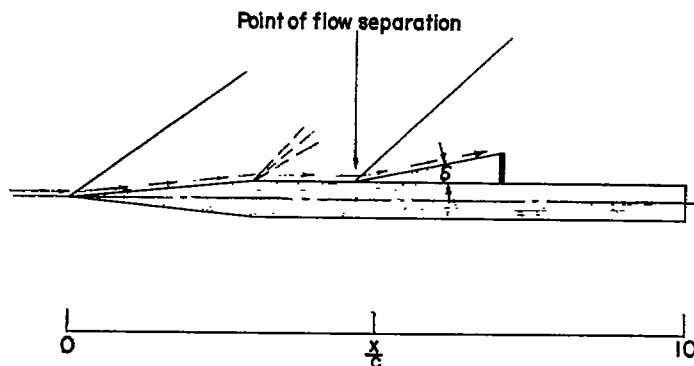


(c) Point of flow separation as predicted by reference 11.

L-77909

Figure 19.- Shock boundary-layer interaction phenomena as depicted by
   schlieren photograph and experimental pressure distribution.  Spoiler
   height, 0.05c; spoiler location, 0.70c; R = 1.87 × 10^6.